

# Politecnico di Torino

Corso di Laurea Magistrale in  
Ingegneria Biomedica

Tesi di Laurea Magistrale

## Studio dell'impiego di fibre ottiche biorisorbibili per il rilascio e la fotoattivazione di farmaci



**Relatore**

Prof. Janner Davide Luca

**Candidato**

Sharon Russo

Ottobre 2022



# ***Contents***

<b><i>Introduction</i></b>	<b>5</b>
<b><i>1. Calcium Phosphate Glass based Fibers</i></b>	<b>7</b>
1.1 Phosphate glasses and optical fibers in Biomedicine	7
1.1.1 <i>Biomedical applications of phosphate glasses</i>	8
1.1.2 <i>Biomedical applications of optical fibers</i>	12
1.2 Fabrication and characterization of the materials	18
1.2.1 <i>Optical fibers structure and propagation of light</i>	18
1.2.2 <i>Calcium phosphate glasses fabrication and characterization</i>	22
1.2.3 <i>Calcium phosphate fiber fabrication and characterization</i>	27
<b><i>2. Bioresorbable core/cladding and hollow fiber</i></b>	<b>33</b>
2.1 Bioresorbable fiber splice to silica fibers	33
2.1.1 <i>Cleaving and splicing</i>	34
2.1.2 <i>Characterization of fiber splice</i>	43
2.2 Fiber and hollow fiber behaviour in PBS solution	49
2.2.1 <i>Dissolution test</i>	50
2.2.2 <i>Angle cut</i>	51
2.2.3 <i>Transmission study</i>	54
<b><i>3. Results</i></b>	<b>57</b>
3.1 Dissolution test	57
3.2 Angle cut	62

3.3	Transmission study	73
<b>4.</b>	<b><i>Biomimetic phantom for fluorophore release</i></b>	<b>79</b>
4.1	The fluorophore molecule	79
4.2	Fabrication of the biomimetic phantom	82
<b>5.</b>	<b><i>Conclusion</i></b>	<b>85</b>
<b>6.</b>	<b><i>References</i></b>	<b>87</b>
<b>7.</b>	<b><i>Acknowledgements</i></b>	<b>91</b>

# Introduction

With the development of optical technologies towards the biomedical field, optical fibers have been explored for different medical purposes such as phototherapy, optogenetics, laser surgery, imaging and bio-sensing.

The ability of fibers to provide light in deep tissues, being minimally invasive, and their unique characteristics have paved the way for the manufacture of optical fibers made of biocompatible and bioabsorbable materials.

In this thesis, the use of optical fibers and hollow fibers based on calcium phosphate glass is studied and discussed.

Starting with the calcium phosphate glass synthesis process, which has excellent optical properties and can safely degrade within the human body, the fiber and hollow fiber production process is explored by focusing on the preform manufacturing and drawing as a fiber of micrometric dimensions.

The fiber and the hollow fiber behaviour in a simulated biological environment was studied.

PBS was chosen as means of miming the human body conditions since it's a buffer solution that helps maintaining a constant pH value and has an osmole concentration that makes it isotonic to the human body.

Through different tests, it was studied how the diameter of the fibers and of the hollow fibers was reducing while these were soaked in containers filled with PBS solution.

The effect of the degradation process on light transmission was studied through a transmission test. While the fiber was soaked in PBS, connected to a laser diode in the infrared region, it was measured the output power coming from the fiber end, for a period of 21 days.

The change in the shape of sharp tips, obtained both in the fiber and hollow fiber samples through an angled cleaving process, was observed, to evaluate if the tips could become rounder while degradating. All tests were carried out by keeping the samples soaked in PBS solution at the temperature of 37 ° C.

At the end of the work, a 3D printed phantom was realized for a further study in which it will be used to observe the release of a fluorophore molecule, using the functionality of the hollow fiber to release drugs.

This type of fiber structure allows to deliver both drugs and light using respectively its hole and wall. The hollow fiber will be filled with Crystal violet fluorophore and this will be released into the phantom. The fluorophore will be excited by delivering light through the bioresorbable fiber spliced to the light source, which is a fiber coupled led at 554 nm.



# 1. Calcium phosphate glass based fibers

In the last years , calcium-phosphate fibers have been deeply studied as promising instruments for different applications. This type of fibers applications have been exploited mainly in biological environment for the singular properties they combine of both calcium phosphate glasses and optical fibers. In this chapter, both the glass and the fibers, that were used in this study, are presented first separately as structures with their story in the optical and biomedical field and then combined together to expand their possibilities and applications on the human body for therapeutic scopes. Starting, the phosphate glasses and the optical fibers are presented in the biomedical scenario with their applications and peculiarities. Moreover, the optical fiber structure and fiber capability of guiding light through it, using optic phenomena and the structure itself, is discussed. Finally, the realizations of the calcium phosphate glasses, the calcium-phosphate fibers and hollow fibers are presented and characterized underlining their optical and biological properties which makes these fibers so important in biomedicine.

## 1.1 Phosphate Glasses and Optical Fibers in Biomedicine

Phosphate based glasses are a group of materials which have unique properties in biomedical applications and offers great opportunity for research and future exploitation.

In tissue engineering phosphate glasses have moved from passive inert implant materials to active biodegradable materials. The main advantage of these materials is the controllable degradation kinetics coupled with ion release rates and cytocompatibility, that can be tuned by varying their compositions. These glasses have at least one terminal oxygen atom in their structure , which is responsible for this particular properties. [1] [2]

In the last years, phosphate glasses have been exploited for a variety of different applications such as hard water treatments, pigment manufacturing, nuclear waste host, solid state electrolytes and laser applications with phosphate glasses doped with neodymium. [3]

Optical fibers, instead, are flexible and transparent fibers obtained [4] by drawing a material, to achieve diameters of the orders of micrometers. Fibers are commonly employed to transmit light between two ends in fiber-optic communications where data transfer rate has a higher value than the one with electrical cables. Optical Fibers are immune to electromagnetic interference so are preferred over metal wires. Their structure with a core cylinder surrounded by a cladding material, with a lower

refractive index than the core one, allows fibers to guide light through their core material using the total internal reflection phenomenon and so to work as waveguides. Fibers can be constructed to admit different propagation paths for light and in particular two types of fiber will be presented and these are single mode fibers and multimode fibers. These properties made fibers suitable structures for applications in biomedicine, where light gained an important role for different therapies as for cancer treatments but also for diagnostics and imaging.

### ***1.1.1 Biomedical applications of phosphate glasses***

The story of calcium phosphates in medicine began in 1769 with the discovery of this material in the bone tissue. This event opened the study of the bone tissue regeneration process and that's why in bone tissue engineering calcium phosphate had its greatest success.

In the last decade, this material has found new fields of interest and been studied for drug delivering devices, for hard and soft tissue engineering, for radiotherapy in the treatment of cancer. Moreover, phosphate based glass's ability to be doped with different ions and to be manufactured in different geometries like fibers, discs and microspheres, opened up to many other applications. [2]

#### ANTIMICROBIAL EFFECT

One application of phosphate glasses (PG) is their use as antimicrobial materials. It was demonstrated that phosphate glass doped with silver had an effective activity against different pathogens like *Staphylococcus aureus*, *Escherichia coli* and *Candida albicans*. [4]

Moreover, PG doped with quaternary gallium showed a great bactericidal effect against Gram-negative and Gram-positive bacteria thanks to the release of the  $Ga^{3+}$  ions.

The copper doped calcium phosphate glasses have demonstrated to be effective both for antibacterial activity and for bone regenerative process.

The release of  $Cu^{2+}$  ions has a bactericidal effect against *S. aureus*, which is a bacteria commonly found in postsurgery infections and is capable of increasing the number of osteoblast cells. [6] [5]

## POROUS MICROSPHERE

Microsphere showed beneficial effect in biomedical application because of their delivery with a minimal invasive injection. For example, microsphere can be used instead of scaffold to fill a defect. Phosphate microsphere doped with  $\text{TiO}_2$  were used to test cell culture using MG63 cells and this study showed that microsphere are a good surface for cell attachment, growth and proliferation.

Porous microspheres still can provide better distribution of drugs, cells and growth factors by controlling the size and the shape of pores. Phosphate glass formulation into microsphere with interconnected pores was recently build via flame spheroidization process. The porous structures size can be different according to the destination of use of the microspheres. Bigger interconnected pores can be used for a faster access of fluids into the microsphere or to promote cells proliferation while smaller pores can be used to withheld drugs or othe substances controlling their release. [5]

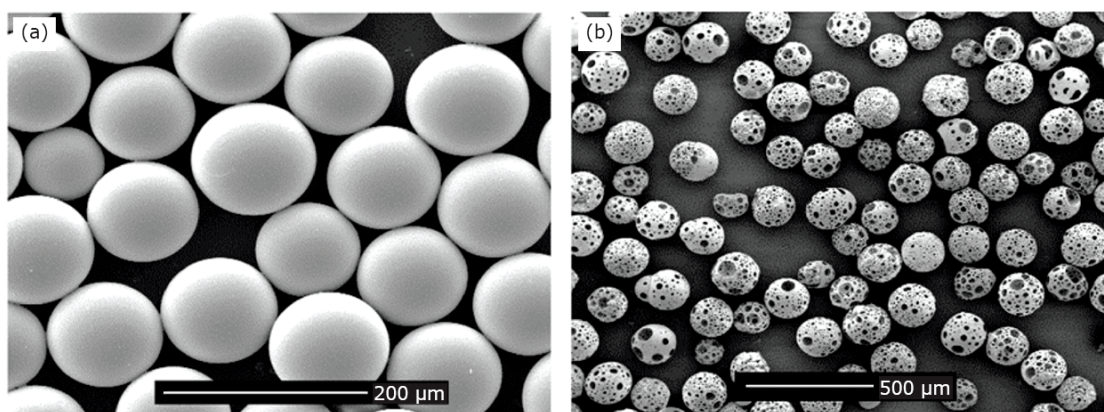


*Figure 1 : (a) bulk microspheres; (b) porous glass microspheres [5]*

## PHOSPHATE GLASS FIBERS

Phosphate glasses in the form of fibers have showed high cytocompatibility and mechanical strength. For these characteristics, they have been explored for biopolymer matrices reinforcing and for soft tissue regeneration.

In the first case, phosphate glass fiber have been developed to match in particular to the mechanical properties of bone. In bones, longitudinal mechanical properties are higher than those in the trasverse direction. PLA plates reinforced with different fibre content and geometries were produced and tested but these composites showed

high reduction of mechanical performance when immersed in aqueous media. They later have been explored via in situ polymerization process. In this way, composite's mechanical stability was increased in its flexural strength e modulus. [6]

In *soft tissue engineering*, phosphate glass fibers have been explored, for example, to guide axonal growth in spinal cord injury. Phosphate glass fiber scaffolds were implanted in a rat in the proximal and distal stumps after a complete transection of spinal cords at T9 and compared to phosphate glass free-collagen scaffold also implanted but in the transected spinal cords of the control group. After implantation axon growth was observed from the proximal and distal stumps but not in the control group. [7]

In another work, phosphate glass fibers have been studied to treat peripheral nerve injuries. These injuries can cause total loss of motor and sensory functions in a particular body area. A series of phosphate glass with different concentrations of  $\text{TiO}_2$  were synthesized and drawn in fibers. This type of glass has showed a good compatibility with osteoblasts cell. It was performed a dissolution test to study the dissolution rates of the different glass composition and then biological tests. These fiber have proved to maintain a structure and composition integrity during degradation and that the increasing in concentration of  $\text{TiO}_2$  stabilize the glass, decreasing the solubility.

From biological tests was proved that these fibers helps improving adhesion of glial cells and support axonal growth. [8]

## PHOSPHATE GLASS HOLLOW FIBERS

Hollow fibers had a great impact in medical field for therapeutic scopes. The inner lumen of hollow fiber can be used to deliver drugs to target site, to promote cell culture and for blood purification. [9]

One relevant work with calcium phosphate hollow fibers was conduct to study the delivery of four different drugs and the interaction between ionized and neutral molecules with the inner glass surface. The drugs selected for this study were caffeine, theophylline, salicylic acid and procaine. These molecules, all with different chemical-physical and pharmacological activity, were chosen to observe different interactions with the inorganic glass surface.

The dissolution test performed showed a complete dissolution of the hollow fiber in 21 days with pH value always in physiological range and release of all the drugs in 18 minutes but with different release profile. At pH of 7.4, salicylic acid and procaine are present respectively in anionic and cationic form while theophylline

and caffeine molecules are in neutral form. It was showed that the ionized species had the tendency to form hydrogen bonds with the glass wall, due to the presence of P-OH groups in the composition of glass and tend to be withheld for a longer time. [10]

Later, the same procedure was repeated to observe the release of two different photosensitive drugs for Photodynamic Therapy (PDT).

PDT has been studied to treat tumor by binding particular photosensitizer to the cancer cells. The need of delivering these drugs in the site of interest brought to the use of Calcium Phosphate hollow fiber to both deliver drugs and light. Rose Bengal and Methylene Blue solution with PBS were released studying the interaction of these drugs with the glass.

Methylene Blue showed strong interaction with the glass surface while the Rose Bengal was completely released in 15 minutes.

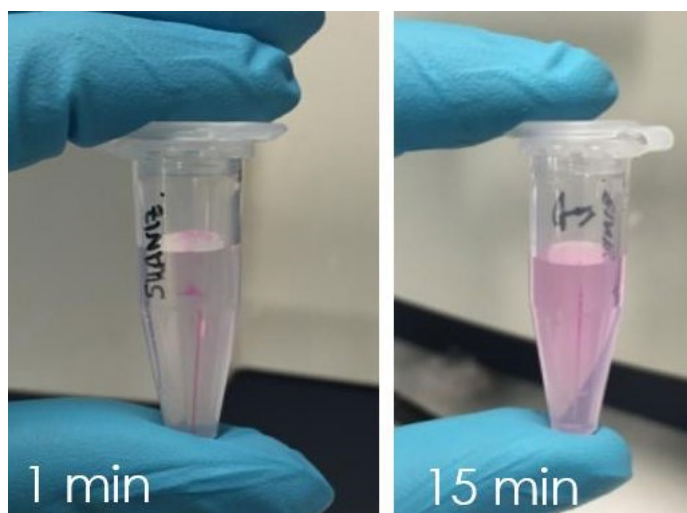


*Figure 2: The release test in PBS of Rose Bengal from a capillary sample filled with it and soaked in the solution*

## ***1.1.2 Biomedical applications of optical fibers***

Optical fibers are used in telecommunication, sensing and lighting field since a long time. With the development of optical technologies towards medical applications, optical fibers have been studied for different medical purpose such as phototherapy, optogenetics, laser surgery, stimulation and imaging. The ability of fibers in delivering light in deep tissues allows to overcome the limit of light's penetration depth in biological tissues. In fact, in Visible/Near Infrared region, the penetration depth of light is less than 3 mm, due to light absorption and scattering.

In this scenario, fiber and waveguides that were biocompatible and bioresorbable, which means they could degrade safely in physiological conditions, started to be very auspicious.

The impact of implantable fiber and waveguides on human body demand to consider particular fabrication and biocompatibility aspect, such as mechanical properties according to the site of implant, low cytotoxicity and biodegradability.

Silica quartz fibers, which are very common in telecommunication field, have been used in different medical applications for their excellent optical properties. Their high optical transparency, low propagation losses and their chemical inertness makes them suitable material to design implantable devices. However, their stiffness might cause wounds when implanted in a biological tissue and this lead to poor biocompatibility.

Organic materials, as silk and cellulose, have been later explored for their high biocompatibility and biodegradability but still their optical properties were not comparable with those of inorganic materials. Compared to silica fibers, these materials have much higher propagation loss.

Synthetic polymers have been explored for their easy processing and their degradation in aqueous media that can be controlled by their molecular weights and different chemical composition. PLLA, for example, has high refractive index and good transparency that make it suitable to guide light in deep tissue. [11]

In this thesis, the study of the use of optical fiber in biomedical field was carried out using fibers formed by a novel material, used for bioresorbable optical applications, which is a variation of the previously presented phosphate glass and this is the *Calcium-Phosphate Glass*. Thanks to the high transparency and biodegradability, controlled by changing the composition of the glass itself, this material is a good compromise between the excellent optical properties of glasses and the biocompatibility properties of organic materials.

Before focusing on these type of fiber and on their study we see now some relevant applications of optical fibers.

### OPTOGENETICS

In *optogenetics*, the study of neurons and their behavior can be done using optical fibers to deliver light in targeted cells to activate or deactivate some particular events . Optogenetics combines optical and genetic methods. Compared to electrical

stimulation which can only target neurons of a specific brain regions, the optical stimulation target specifically neurons that express opsins protein.

The gene that make neurons express opsins is carried to specific cells by a viral vector , which is injected in the specific brain area, and encodes a particular protein that is responsible for electric current in cells membrane with light excitation.

Recently, the possibility to create optical fibers capable of performing several functions became very auspicious. Some polymer fibers have been realized with a coating made by silver nanowires to simultaneously record electrophysiological activity and to stimulate neurons. Other fibers have been later created with micro channels to include also the ability of delivering the viral vector. [11]

Optical fibers made of PLLA material are common tools for optogenetic studies and researches. PLLA is a bioresorbable and biodegradable synthetic polymer with an high transparency in the visible range and an higher refractive index than tissues that makes these fiber capable of delivering light in deep tissues. Some studies, performed with these type of fibers on living mice, showed the high potential of optogenetics for in vivo applications and in vivo sensing with the gradual degradation. [11]

## PHOTODYNAMIC THERAPY

The importance of light in therapy treatment for cancer, in optical diagnostics and photodynamic therapy have lead to great influence of lasers and optical device on medicine.

By selecting some specific light wavelengths, different clinical practice can be achieved.

*Photodynamic Therapy (PDT)* is nowadays a chosen treatment for some types of cancers like head, neck, lung, bladder and skin malignant cancers. It combines the delivery of photosensitizer drugs, designed to destroy cancerous cells, and the light delivery. With this strategy, photodynamic therapy is capable of targeting and destroy only the diseased cells without damaging the healthy cells. Implantable fibers improves the therapeutic delivery of light depth in these therapies allowing the treatment in deep tissues. [11]

PDT is used also in treating acne, psoriasis and macular degeneration. It is minimally invasive technique and also a low toxicity one.

It is a multi-stage process that involves: the delivery of the photosensitizer drug, locally or systemically, later when the concentration of drug is enough in the target tissue, light is activated and delivered by the optical fiber for an exposure period. The light source must be appropriate for the chosen photosensitizer, which means it has to make it produce radicals or reactive oxygen species that will kill the target diseased cells. The light dose is enough to stimulate the drug but not to damage the healthy cells.

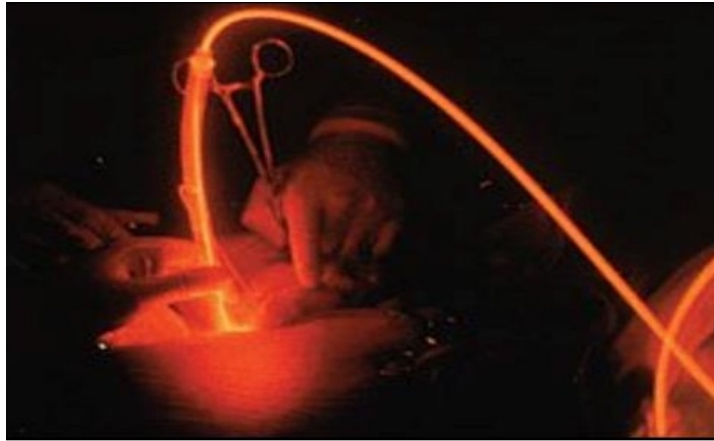


*Figure 3: Example of photodynamic therapy [11]*

### PHOTOCHEMICAL TISSUE BONDING

Optical waveguides are used to perform *photochemical tissue bonding* (PTB) , which is a technique employed to repair tissues and to close wounds. PTB works using a light sensitive dye and applying light to the tissue. The dye absorb the light and cause the crosslinking of the tissue forming a water tight seal. Thanks to optical waveguide light is capable of reaching higher penetrations depths.

In a study, Rose Bengal dye has been used combined with green light to seal a wounds on a porcine piece of skin. Rose Bengal absorb the light wavelengths of the green light. The penetration of light has been achieved thanks to a polymeric comb slab which is pigtail fiber coupled to the laser source and after implant and light emitting it is simply cut off leaving within the closed wound, the biodegradable waveguide. [12]

In another study, PTB have been tested for ppheripheral nerve repair for a minamilly invasive repair in the site of interest. The epineurium is suited for Photochemical technique because its thinness and high content of collagen. The study showed axonal regeneration with no difference with respect to the gold standard. [13]

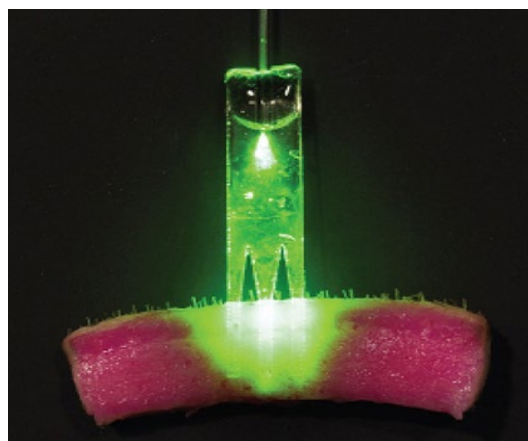


*Figure 4* : Example of photochemical tissue bonding using Rose Bengal dye and green light on a pig dorsal skin [12]

## FIBER OPTIC IMAGING

Optical imaging is the tool that allows to investigate the biological environment and to diagnostic disease. It uses light to obtain detailed images of organs, tissue and cells. This technique is minimally invasive allowing to detect also deep region of the body.

Optical imaging does not use ionizing radiation but it uses visible, ultraviolet and infrared light which are much safer for the patients. [11] Endoscopes applications can involve the use of fibers that can be inserted inside the body to inject light and to collect the light reflected back from the surrounding tissues reproducing in this way an image of the inside of the body that was previously illuminated.

Implantable optical fibers for the delivery of light and to collect information are efficient tools that allows a long time monitoring and good resolutions. Light is transmitted from one end to the other of the fiber transmitting only the light that comes from that part of the image. Keeping the configuration of the fiber constant, the light will form an identical image at the other end of the fiber.

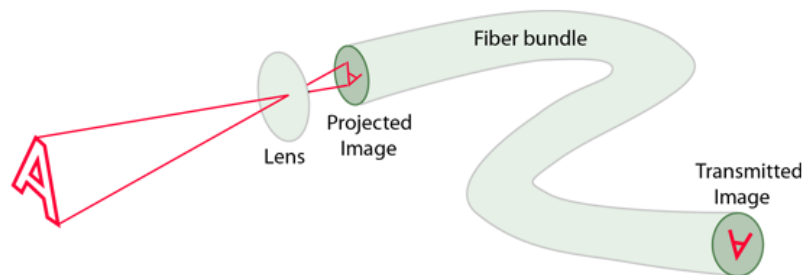


*Figure 5: Optical imaging scheme*

## OPTICAL SENSING

Optical Sensing is a technique that uses the properties of light, guided by optical fibers, to detect changes in measurement as temperature, strain, current, detection of bio-molecules and many others. Optical sensing exploit the small dimensions of the fibers combined with their chemical inertness, linearity and the high sensitivity.

It can be used to get information about biological activities, for rapid diagnostic of disease and for real time monitoring in industrial or pharmaceutical applications.

In biomedicine, for example, optical fiber sensors have been employed as glucose sensors because of the have high impact of these devices on diabetes diagnosis, monitoring and detection. Glucose sensors are also the most important part for an artificial pancreas which controls the insulin release thanks to these sensors.

The sensor consist of a proper light source, two optical fibers made of PMMA (polymethylmethacrylate) connected togheter and a photodiode detector. Light is launched in the fiber and its properties are used to detect variations of refractive index with the concentration of glucose in distilled water. The results show that the refractive index of the medium increases linearly with the glucose concentration in solution. [11]

In another study, hydrogel fibers were used for optical sensing of blood oxygenation. Two of these fibers were implanted in an anesthetized mouse in subcutaneous tissues, one for delivering excitation at 560 and 640 nm and the other to collect the light emission and to measure the optical absorption signal in response to a nitrogen/oxygen ventilation. The nitrogen inhalation caused a drop of oxygen in blood, increasing the deoxyhemoglobin and decreasing the oxyhemoglobin concentrations.

These discovery increased the potential of optical sensing for vivo and real time monitoring in photomedicine field. [11]

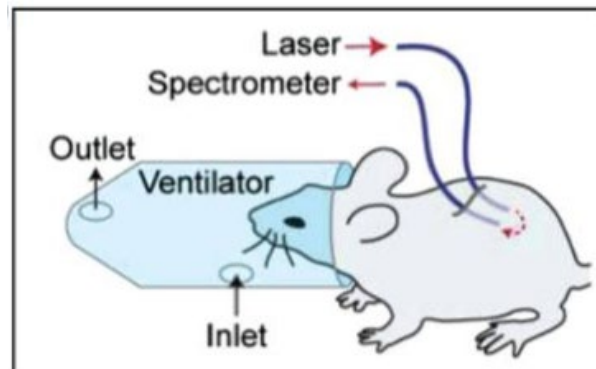


*Figure 6 : Rapresentation of the absorption spectroscopy on a mouse [11]*

Moreover, Fiber Bragg Grating (FBG) is a technology which become nowadays the most common real time sensing method used in optical fiber. Fiber Bragg grating system is mostly used because of its non toxicity, chemical inertness and immunity to electromagnetic interferences for detecting variations of physical parameters such as temperature, pression, refractive index or strain.

FBG is a microstructure created inside the core of a single mode fiber by photo inscription which is a technique that involves the use of a mask to create an interference pattern in the core section by illumination of the fiber with a UV laser beam source.

This operation will create a spatial periodic modulation of the core refractive index, making the core a resonant structure. The FBG appears as a notch filter that will reflect back only the light within a narrow band of wavelengths centered at Bragg wavelength. The other part of light will be transmitted without losses. [14] In FBG biosensing devices the variation of refractive index at the interface between fiber and the biological environment is related to the recognition of a biochemical species. For diagnostic, the immobilization on the fiber surface of antibody, nucleic acid or whole cells can allow to capture the respective target as proteins, virus or whole cells. This devices have been largely explored for a rapid diagnostic of genetic diseases, bacterial infections and tumoral biomarkers. [15]

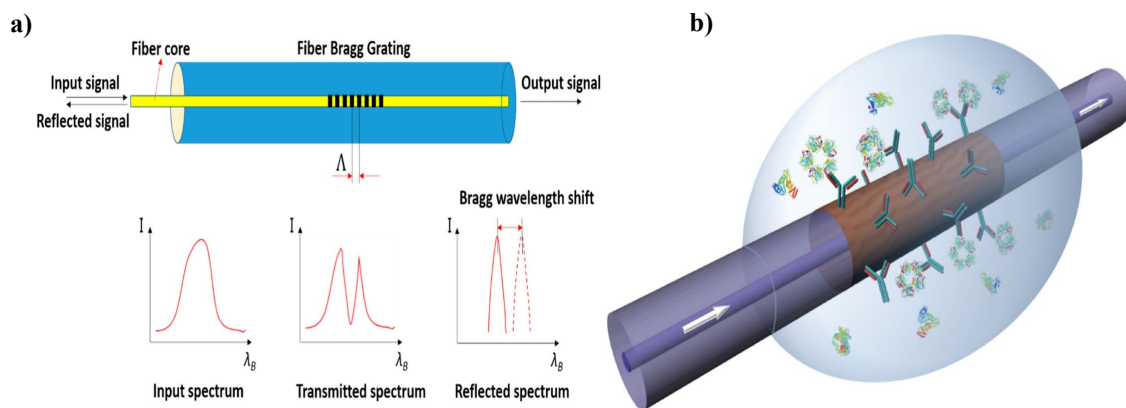


**Figure 7:** a) *Fiber Bragg Grating working principle [14]* b) *Fiber Bragg Grating for recognition of biomolecules using antibodies immobilized on the surface. [15]*

## 1.2 Fabrication and characterization of the materials

In this section, the fabrication of the calcium-phosphate glass samples, of fibers and hollow fibers is presented. Before discussing this part, it is important to explain how optical fibers are structured so to understand better some fabrication and characterization aspects of the glasses.

We first focus on the fibers structure, going into detail on the phenomena that combined with the particular fiber structure, made of core, cladding and coating structures, allow them to guide light inside of them.

Later, the fabrication of the glasses used in this work is introduced focusing on the preparation of the glass samples for core and cladding structures of the fiber and for the hollow fiber, with different compositions and through different preparation methods.

Finally, the fabrication of the preform of the fiber, the drawing process of the preform and the characterization of the calcium phosphate fiber is deeply explained. Calcium-phosphate hollow fiber fabrication and characterization is also discussed, focusing on its type of employment in this study.

### *1.2.1 Optical fiber and propagation of light*

In fiber optic, light propagation through fibers is due to different characteristics of light like refraction and total internal reflection. To better understand these concepts is important to know the basic structure of a fiber.

An optical fiber is composed of three parts: the core, the cladding and the coating. The core is a cylindrical rod of dielectric material, is usually made of glass and has a refractive index  $n_{\text{core}}$ . Dielectric materials do not conduct electricity so they are suitable material for both core and cladding structures. The cladding is the surrounding material of the core and must have some specific requirements. To confine light in core, where it usually propagates, the cladding must have a refractive index  $n_{\text{cladding}}$  lower than the core's one. The cladding is also useful because it reduces both the loss of light from the core into air and the scattering loss at core's surface, it protects the fiber from contaminants and increase its mechanical strength. The cladding can be surrounded by an additional layer called coating to protect fiber from physical damage and which is usually made by a polymeric material. It also prevents the fiber from scattering loss due to microbends. [16]

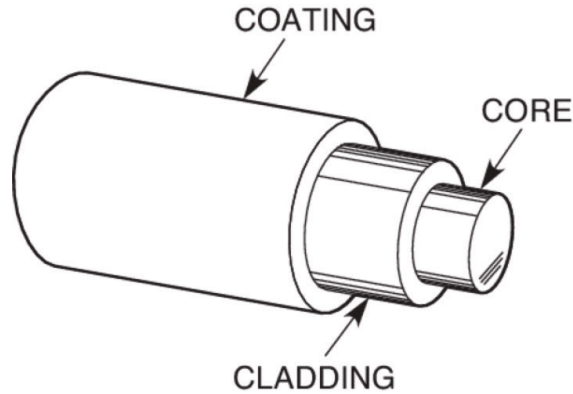


*Figure 8 : Optical fiber composed by three different layers [16]*

The fiber structure plays in this way an important role in the refraction and total internal reflection phenomena thanks to which light guidance is achieved. The refraction phenomena appears when light goes from a denser medium to a rarer one or vice versa, the light propagation's direction changes at the interface between the two medium. The refractive index is a measure of medium's density so it is higher for a denser medium. The angle between the incident ray and the normal is called angle of incidence, while the angle between the refracted ray and the normal is the angle of refraction. As shown in **Figure 9** when light goes from a denser medium with higher refractive index to a rarer one with lower refractive index, the angle of refraction is greater than the angle of incidence. The opposite situation is founded when light goes from a rarer medium to a denser one.

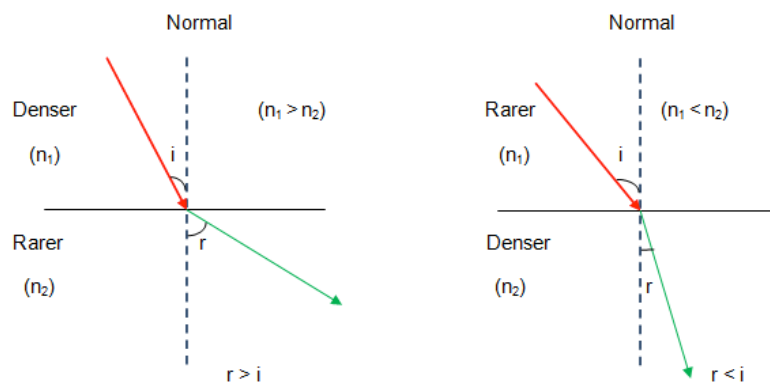


*Figure 9: Refraction between different medium in two situations*

When light propagates as in the first case, from denser to rarer medium, if the angle of refraction is  $90^\circ$  then the angle of incidence is called critical angle. If a light ray is incident at the interface with an angle greater than the critical angle this is completely reflected back to the denser medium. This phenomenon is called total internal reflection. [17]

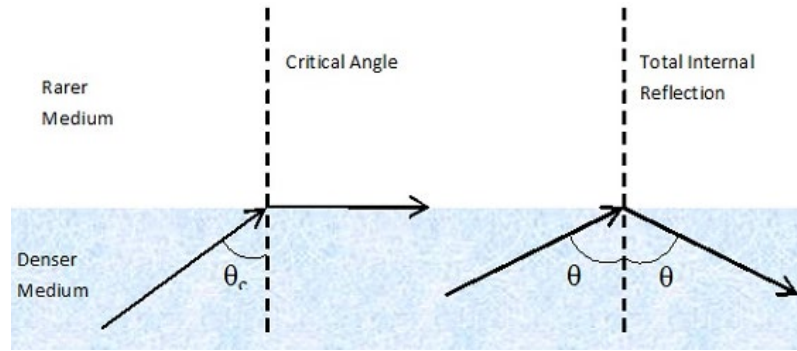


*Figure 10 : Total Internal Reflection phenomenon*

Total internal reflection is used, in optical fibers, to transmit light in fiber by confining it in the core section.

The core is made of a denser glass with higher refractive index than the cladding's glass which is less dense and with lower refractive index.

Because of that, when light pass through the core it is reflected back and not refracted to the cladding. However, imperfections at the core-cladding interface will cause some light to be refracted in the cladding and escape from the fiber. [17]

Moreover, rays that enter in the fiber must intersect the core-cladding interface at an angle greater the the critical angle to have the total reflection in the core, only those that enter the fiber at these values of angle will propagate along the fiber. The light rays incident on the core, to propagate in it, must be within the acceptance cone. The acceptance angle is the maximum angle to the axis of the fiber that makes light propagate in core and is related to the refractive indeces of the core, cladding and the surrounding medium. This relationship is explicated by the Numerical Aperture value (NA) , which is a measure of how much light the fiber can capture. This measure relate the refractive index  $n_1$  of the core to the refractive index  $n_2$  of the cladding to the one of the surrounding environment  $n_0$ . Using Snell's law and trigonometric relationships we have:

$$NA = n_0 \times \sin \theta_{max} = (n_1^2 - n_2^2)^{1/2} \quad (1.1)$$

Since the surrounding medium is typically air,  $n_0$  is equal to 1 and NA is simply equal to the sin of  $\theta_{max}$  which is the acceptance angle (**Figure 11**). [18]

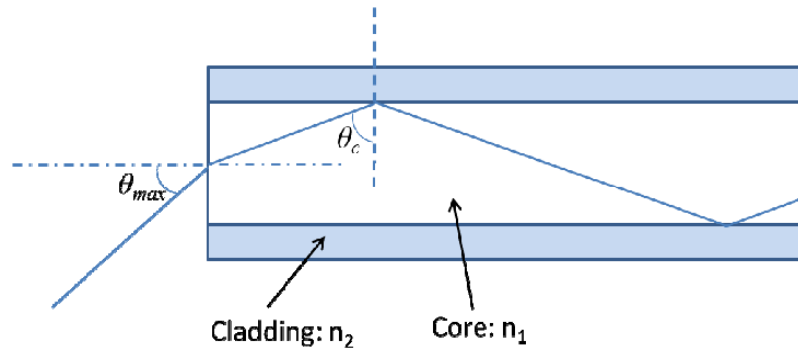


Figure 11 : How light rays enters an optical fiber [18]

Optical Fibers are classified by the number of modes of light that can be propagated in the fiber. Basically, it depends on different core's size. The first type of fiber is the **Single Mode Fiber** that makes light propagate only in one mode because core's size is very small and has typically diameter values around 8 to 10 micrometers. Single mode fibers, whose core dimension is less than ten times the wavelength of light, cannot be explained by the geometric optics but they are explained as electromagnetic waves according to Maxwell's equations. The second type of fiber is the **Multimode Fiber** which allows multiple beams from the light source to move along different paths. The core size is bigger with diameter values from 50 to 62.5 micrometers. This type of fibers can be described by the geometric optics because of the core's higher dimensions. [19]

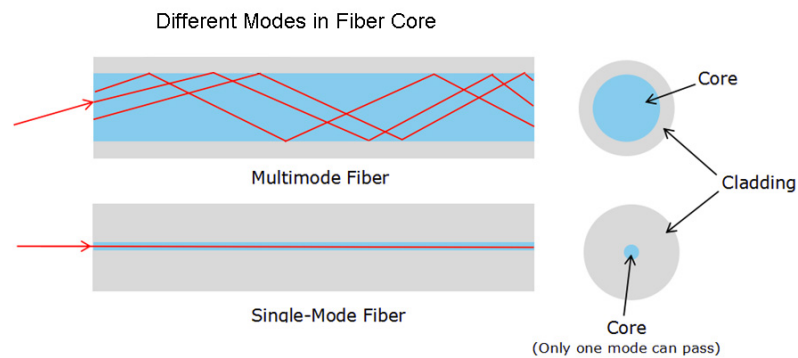


Figure 12: Multimode Fiber and single mode fiber [20]

Optical fibers have to deal with losses or attenuation losses, that are measures of the amount of light lost from the input point to the output. The causes of fiber losses are different and can depend on the material absorption or bending. Losses are categorized as intrinsic optical fiber losses or extrinsic ones depending on the cause.

Intrinsic losses are due to structural defects and include absorption, dispersion and scattering losses. Extrinsic losses are due to external causes and include bending and splicing losses. The total attenuation is the sum of all type of losses and is expressed in dB/m.

The fiber's attenuation coefficient  $\alpha$  can be calculated by measuring with a power meter the input power  $P_0$  and the output power  $P_L$  on a fiber of length  $L$  using the expression :

$$\alpha = \frac{10}{L} \times \log_{10} \frac{P_L}{P_0} \quad (1.2)$$

When light propagates in a transparent medium, part of its optical power is lost due to intrinsic and extrinsic losses. [20] Propagation losses are caused by :

- Some light is absorbed by the material it self and generally converted into heat because of the interactions between lightwave and component of fiber's material. For a particular fiber , these losses depends on the chosen wavelength of light and on the manufacturing material.
- Light can be scattered while it propagates and sent in other directions. These type of losses doesn't reduce the total amount of light but just the quantity of light in the original direction.
- Light can be lost also because of mode coupling that causes a transfer of power from the guided modes to the unguided modes, this can be caused by strong mechanical stresses, like the bending of the fiber. [21]

When two or more fibers are joined together by fusion splicing technique that will be deepen in the next chapter , optical power loss at the splice point is called splice loss. Also these losses can be caused by extrinsic or intrinsic parameters.

Intrinsic parameters includes differences in core diameter and numerical aperture of the fibers that can be limited adjusted by a proper alignment method.

Extrinsic parameters are related to the splice procedure and its settings. These include wrong alignment, contamination of fiber end, bad end cleaves and core deformation caused by a wrong heating power or pressing. [22]

## ***1.2.2 Calcium Phosphate Glass fabrication and characterization***

Calcium phosphate glasses (CPGs) have raised great interest, in recent years, in field of biophotonics, optogenetic and biosensing.

The aim of researcher was finding a compromise between biological features and technological properties in an optical device that could be also designed to be fully resorbed once found in an aqueous media. The CPGs was the first type of

phosphate glass designed to be completely resorbed modifying the composition of the glass itself so to control the dissolution kinetics. Thanks to their optical properties and the high optical transparency in the UV-Visible/Near Infrared region, from 250 to 2500 nm, calcium phosphate are suitable glasses for applications in photomedicine.

The properties of phosphate glass comes from its tetrahedron structural unit  $PO_4^{3-}$  with three bonding oxygens linked to the near structural unit and a terminal oxygen linked to the phosphorous atom. [23]

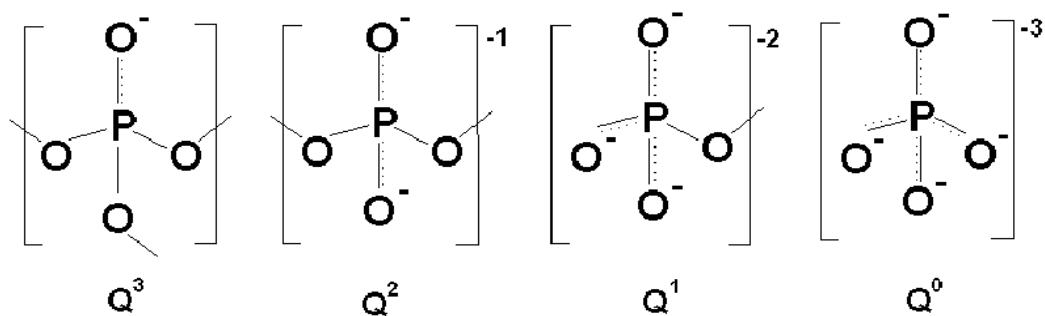


*Figure 13 : Phosphate glasses tetrahedral structures*

The number of bridging oxygens present in the tetrahedra structure determine a range of different structures, from  $Q^3$  to  $Q^0$ . These structures effect some properties of the material such as transition temperature, refractive index and dissolution kinetics.

In particular, calcium-phosphate glasses dissolution behavior is modified by the presence of MgO and CaO oxides in the glass composition. Higher is the concentration of MgO, more the glass network is stabilized by the strong bond between  $Mg^{2+}$  cations with the non-bridging oxygens of two different chains, decreasing the dissolution speed of the glass.

The  $Mg^{2+}$  divalent cations forms a stronger ionic-crosslink than the  $Ca^{2+}$  ones because of the smaller ionic radius and so a stronger field than  $Ca^{2+}$  that has an higher radius. [24]

The glass samples used during the work of this thesis were of two types, one composition was developed for the core of the fiber and the other for the cladding. Another unit of the same glass composition of the cladding was fabricated to create a tube, realizing the preform for the hollow fiber.

The core chemicals used were  $50\%P_2O_5 - 30\%CaO - 3\%MgO - 11.5\%Na_2O - 2.5\%B_2O_3 - 3\%SiO_2$  while the cladding chemicals were  $50\%P_2O_5 - 10\%CaO - 23\%MgO - 11.5\%Na_2O - 2.5\%B_2O_3 - 3\%SiO_2$  (in mol%) with purity level of 99 + % .

Silica, magnesium oxide and boron oxides are network formers of the glass, act as building blocks and are basic components to prevent devitrification and improve mechanical stability while sodium, calcium and phosphate oxides are network modifiers and can bond to the non-bridging oxygens. [24]

The cladding glasses can be generally synthesized by rotational casting or extrusion method. The rotation casting is a technique that cast a glass melt into a cylindrical mould, kept in vertical position, that was pre-heated. The mould, in horizontal direction, is rotate at a speed about 300 rpm creating a hollow structure. The mold is later insert in a furnace for glass annealing. This process is very fast, can be performed in few seconds, but tube's diameter dimension is limited and casting temperature and viscosity are important features to control wall thickness and diameter that can be obtained.

The cladding glasses for this study were instead synthesized by extrusion method in Links Foundation. Extrusion facility includes a press mandrel that applies a pressure on a glass billet. The billet is is heated in the furnace zone to reach the extrusion temperature where the viscosity of the glass is about  $10^{5.5}$  and  $10^7$  Pa·s.

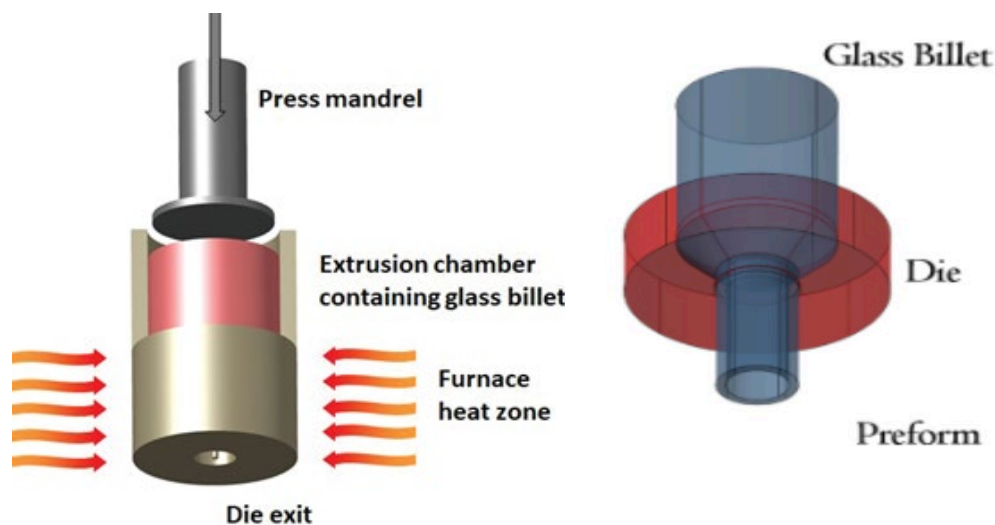


*Figure 14 : Scheme of the extrusion technique [24]*

The furnace is composed by a metallic tube that holds the die while it is inserted in the alumina furnace where is heated by a symmetrical tubular array to reach a circular temperature distribution of the die. The application of the load on the glass billet make it forced to pass, after heating zone, trough an orifice that mimic the final

shape of the preform. At the end of the process we obtain the preform with the diameter reduction expected. [24]

The core's glass, instead, was synthesized by the melt-quenching method.

This procedure requires the mixing of the chemical precursors, which were previously weighted. Most of the chemicals are modifiers oxide combined with the main glass component which is the phosphorous oxide  $P_2O_5$ . Since these precursors are very hygroscopic which means they can adsorb and absorb water from the environment, in order to control the presence of hydroxyl ions they were mixed in a controlled dry atmosphere, in a glove box at 25 °C with humidity value inferior to 0.1% under flux of dry  $N_2$ . The chemicals were melted in alumina crucibles at a temperature of 1200 °C for 1 hour, then the melt was cast into a preheated brass mould and annealed at a temperature close to the transition temperature  $T_g$ , to relieve internal stress, for 12 hours. Finally, it was cooled down to the room temperature. [23]



*Figure 15: Cast of the melt*

The glasses obtained were cut and polished to a thickness of 1 mm for optical and spectroscopic characterization and of 12 and 5 mm respectively for density and coefficients of thermal expansion (CTE) measurements. Compositions of core and cladding suitable for fiber drawing and extrusion requires stability against crystallization, similar glass transition temperatures ( $T_g$ ) and low difference of CTE. Density of glasses was measured by the Archimedes's method using distilled water as immersion fluid, at room temperature, with an error of  $0.005 \text{ g/cm}^3$ . The formula used to calculate the density was :

$$\rho = \frac{W_{dry}}{W_{dry} - W_{wet}} \quad (1.3)$$

Where  $\rho$  is the sample's density,  $W_{dry}$  is the weight of sample in air and  $W_{wet}$  is the weight in water. The coefficient of thermal expansion (CTE) was measured with an alumina dilatometer at 5°C/min on 5 mm long samples until a value of shrinkage higher than 0.13% was reached. The starting of shrinkage concur with the softening temperature ( $T_s$ ) of the glass. Thermal expansion experiments were performed using Netzsch, DIL 402-PC model.

The refractive indexes of glasses were measured directly on the material at different wavelengths: 633, 855, 1061, 1312, 1533 nm, with a Metricon 2010 Prism Coupler with an estimated error of  $\pm 0.001$ . In the following table the refractive indices of the core glass and of the cladding glass for the respective wavelengths are shown. [23] [24]

<b><i>Wavelengths (nm)</i></b>	<b><i>633</i></b>	<b><i>855</i></b>	<b><i>1061</i></b>	<b><i>1312</i></b>	<b><i>1533</i></b>
<b><i>Core Glass</i></b>	<i>1.5269</i>	<i>1.5218</i>	<i>1.5187</i>	<i>1.5158</i>	<i>1.5135</i>
<b><i>Cladding Glass</i></b>	<i>1.5148</i>	<i>1.5102</i>	<i>1.5068</i>	<i>1.5039</i>	<i>1.5017</i>

*Table 1 : Refractive indices for core and cladding glass at different wavelengths*

Differential Thermal Analysis (DTA) was performed using a Netzsch DTA 404-PC model, with a constant heating rate of 5 °C/min, to measure two different characteristic temperatures: glass transition temperature  $T_g$  and the crystallization temperature  $T_x$ .

These two values allowed to assess a glass stability against devitrification and a suitability for fiber drawing with a parameter around  $\Delta T = 200 \pm 6$  °C. The typical error on DTA measurements is  $\pm 3$  °C.

In UV-Vis/NIR range from 180 to 3000 nm, using a double beam Varian-Cary 500 UV-Vis/NIR spectrophotometer, absorption spectroscopy was performed to assess the transparency and UV edge of the glass. The measurements were performed in a single beam configuration. [23]

### ***1.2.3 Calcium Phosphate fiber fabrication and characterization***

Optical fibers used in this work were produced by drawing of a preform, created with rod in tube technique. With this method a small cylinder is insert into a hollow cylinder to form the preform (**Figure 16**). The inner cylinder must have an higher refractive index while the tube has a lower one. The two glasses used for this process are made of the two compositions presented in **Chapter 1.2.2**.

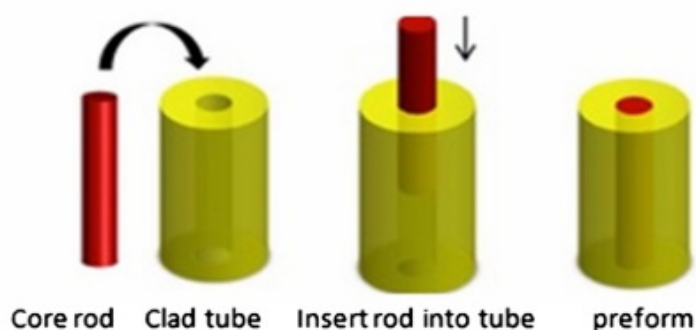


*Figure 16: The conventional steps for rod in tube process*

The preform can be considered as a macroscopic formulation of the final fiber, with the same structure, geometries and the same proportions. Only fiber with diameter ratio of the internal/external cylinder from  $\frac{1}{2}$  to  $\frac{1}{4}$  can be obtained in DISAT laboratory. When the preform is heated in the furnace the two materials both core and cladd are drawn together. To avoid residual stress , the core rod and the clad tube must be carefully polished to reduce defects at the interface between core and cladding.

The drawing of the preform was performed at Links Foundation where is present a drawing tower of 4 meters of height. Typically, drawing towers can reach heights about 20 meters.

The furnace of the tower is a stainless steel ring heated by induction at a frequency of 248 kHz with power from 150 to 250 W to reach the drawing temperature.

The preform is placed in the drawing tower where is heated until the glass reaches a temperature superior to the softening temperature. The effect of gravity and the surface tension forces cause a glass drop forms. The result fiber is then pulled using a capstan or using a rotating drum at the bottom of the tower. The preform dimensions are typically at the mm scale and using high tensions the final fiber diameter and geometry can be controlled.

The fiber diameter is monitored by fixing the speed of insert of the preform and the speed of drawing of the final fiber. Considering the glass as an incompressible liquid when is supercooled it can be applied the mass conservation law and we have:

$$D_{preform}^2 \cdot V_{preform} = d_{fiber}^2 \cdot v_{fiber} \quad (1.4)$$

Where  $D_{preform}$  (mm) is the preform diameter,  $V_{preform}$  ( $\mu\text{m/s}$ ) and  $v_{fiber}$  (m/min) are the speed of the preform and of the fiber while  $d_{fiber}$  ( $\mu\text{m}$ ) is the fiber diameter.

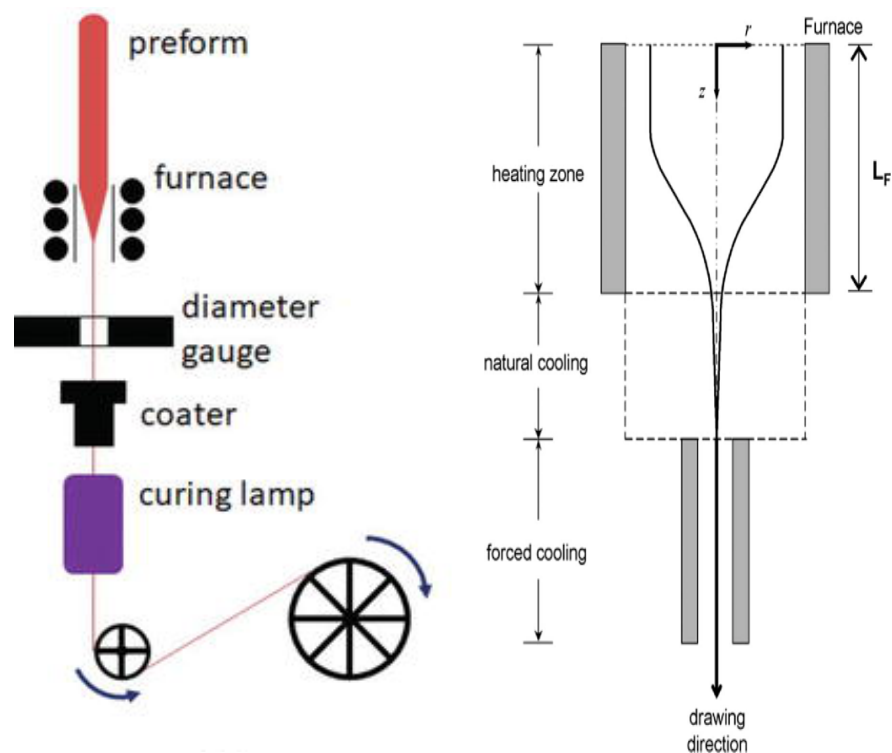


*Figure 17: Scheme of a fiber drawing tower (left) and of neck down zone (right)*

The drawing tower components showed in **Figure 17** are : *the furnace* to heat the preform, *Diameter gauge* to measure the diameter of very small fiber, *the coater* to apply an optional polymeric coating to the fiber, the *curing lamp* is a UV LED light source which cures the coating previously applied to the fiber and the *rotating drum* to collect aligned fibers by controlling its rotation speed. The region were the diameter of the preform reduces drastically is called neck-down (**Figure 17**).

In this region, reached the softening temperature, the material starts decreasing its diameter because of the downward pulling force imposed by the rotating drum and

by the weight of the preform. The parameters effecting the diameter variations are the temperature, viscosity distributions in the neck down region, the neck down shape and the drawing tension. The tolerance for the fiber diameter is  $\pm 3 \mu\text{m}$ . [23] [24]



*Figure 18: Drawing tower facility in Links Foundation*

The characterization of the optical fiber is necessary to assess the quality of the production process and the ability of the fiber to guide light.

The quality is verified with the *morphological characterization*, performed with the optical microscope (Nikon Eclipse 50i) equipped with camera to evaluate the fiber surface, the dimensions and the core and cladding adhesion.

*Near Field Images* were used to assess the ability of the produced fiber in guiding light. Light is coupled to a cleaved end of the fiber and the output was observed with an IR camera.

Both Laser light at 1300 nm and at 633 nm were used to inject light in the fiber sample and take near field images of the cross section to study its modal properties. The *cut-back technique* is usually performed to measure the propagation losses, caused by defects of the glass. This technique is carried on starting from a long fiber sample, the laser was end coupled to one cleaved end of the sample and the output was measured at the opposite end facet with a power meter.

The cut-back is a destructive technique, in fact all these measures were performed in the same way but progressively reducing the length of the sample. The loss values were measured in dB/m.

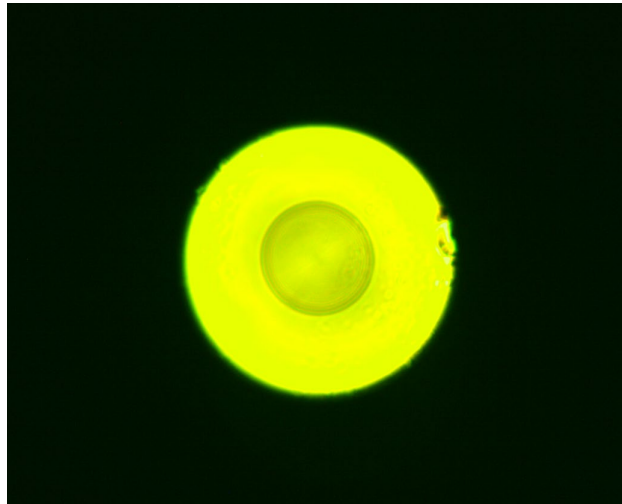


*Figure 19: Cross section view of fiber sample used in this study taken with Optical Microscope*

## HOLLOW PHOSPHATE GLASS FIBERS

The hollow fiber samples used in this work were synthesized by drawing a cylindrical preforms of diameter of 11 mm. The preform consists of a tube with a cylindrical shape realized with the extrusion method. The hollow fiber samples used have a 200  $\mu\text{m}$  diameter. The ability to guide light was assessed launching the light in the hollow fiber with a laser source at 660 nm of wavelength and taking near field images of the cross section. Since this glass is transparent from 260 to 2500 nm the light guidance can be performed in the near UV, in the visible and in the near infrared regions.

Light guiding experiments were performed at different visible wavelength in the red, green and violet region (**Figure 20**). The laser diodes were end-face coupled to a cleaved end of the fiber and the light was observed from the other end with an optical microscope supplied with a camera.

The losses are higher for the hollow fiber due to the presence of the hole and for the missing of core/cladding structures combination.

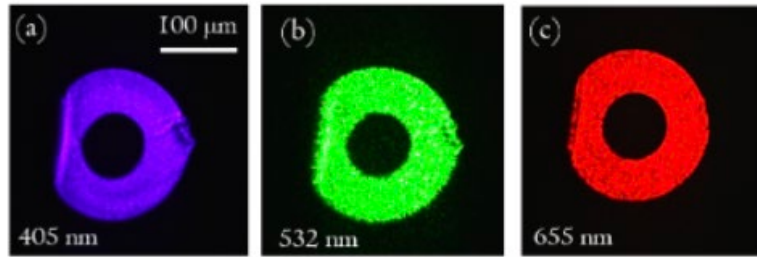


*Figure 20: Hollow fiber guiding light in violet, green and red region [24]*

The main scope of the hollow fiber is the release of drugs combined with light guidance thanks to the total internal reflection phenomenon. In this study its performances in guiding light were studied with a transmission study were one cleaved end of the phosphate hollow fiber sample was not coupled with the laser diode but it was spliced.

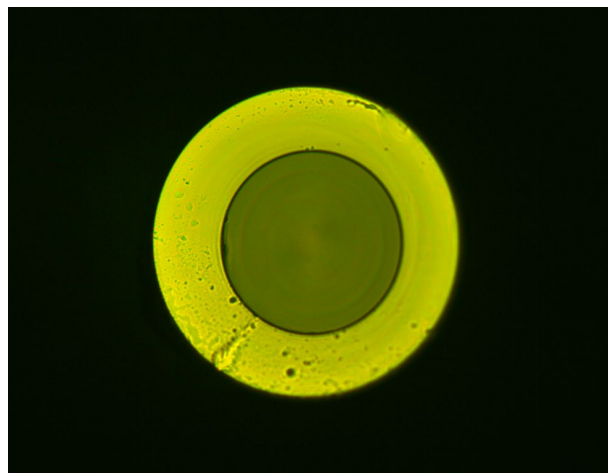


*Figure 21: Cross section view of the hollow fiber sample used in this study taken with Optical Microscope*



## 2. Bioresorbable core/cladding and hollow fiber

In this chapter, we focus on the different tests performed on some samples of Calcium-Phosphate Glass fiber and hollow fiber, whose fabrication and characterization was faced up in **Chapter 1**.

The aim of the study was performing a dissolution test in PBS solution on both fiber and hollow fiber samples to observe their degradation and measuring the diameter reduction in 30 days of experiment.

In parallel, the degradation of the tips of the samples, previously cleaved at different angle, was observed to evaluate if the type of angle at the tip surface could lead, while degradating, to a sharp or a round shape.

Moreover, a characterization of fiber and hollow fiber splice was performed to assess the ability of the samples in guiding light in the infrared region when spliced to a source of light at a specific wavelength.

Finally, a transmission test was also evaluated while the samples were soaked in PBS to examine how the degradation of the samples effected the transmission of light.

To do all these tests, two main processes were necessary to prepare all the samples, which were later studied, and these were the *Cleaving* and the *Splicing* processes.

These two procedures were deeply studied in order to obtain the best results in the guidance of light and a strong mechanical stability of the samples.

### 2.1 Bioresorbable fiber splice to silica fibers

The two type of samples used in this study were the calcium phosphate fiber and calcium phosphate hollow fiber whose samples preparation for all the experiments will be discussed in this section focusing on the cleaving and splicing processes that will be deeply presented.

These two processes were necessary to prepare samples for dissolution, angle cut and transmission study.

In particular, for dissolution test both type of samples were cleaved on both ends with a cleave plane perpendicular with respect to the longitudinal axis of the samples.

For angle cut study, the samples were cleaved so to have particular angle value on one end. Using Fujikura cleaver it was possible to perform angled cleaves by applying torsion with a rotating right clamping stage in accordance with the target angle.

For transmission study both cleaver and splicing were important for a good light guidance.

Cleaver machine was used to obtain the desired angle on both end of the samples and then the splicer used to obtain a good junction in both samples ends, in the first case between calcium phosphate fiber and silica multimode fibers and in the second case between calcium phosphate hollow fiber and silica multimode fibers.

A characterization of fiber and hollow fiber splice will be also presented, in this section, with its experimental setup. This study was need to optimize the splicing process and to observe light guidance with Xeva camera with both type of samples using a laser diode in the infrared region. The bioresorbable samples were spliced on one end with a multimode silica fiber while the other end was left free for camera detections.

The losses dued to propagation of light and to splice were also measured using a power meter to measure the output power coming from the free cleaved end of the fiber and of the hollow fiber samples whose second ends were spliced to the laser source.

## ***2.1.1 Cleaving and Splicing***

The ability of the calcium-phosphate fiber and hollow fiber to guide light was assessed as discussed in **chapter 1** thanks to the Total internal reflection phenomenon and the particular structure of the fiber with a core refractive index higher than the cladding refractive index. In that case the laser diode was coupled to one cleaved end of the phosphate fiber and the same for the hollow fiber.

In this case, the laser diode was connected to the calcium phosphate samples in a different way and in particular through a junction between the two different fibers. The junction, which was realized with a CO<sub>2</sub> Splicer, requires particular characteristics of the two surfaces to allow light to be launched into the fiber in a proper way.

### CLEAVING

Fiber cleaving is an important and standard process in fiber optics for preparing the fiber surfaces in order to obtain, later, a low loss splice.

A cleave is a controlled break in the optical fiber intended to obtain a flat surface or a surface with a particular angle with respect to the longitudinal axis of the fiber. The method employed for cleaving is called scribe- and- tension strategy.

It consist in creating a scratch in the fiber in a particular site of its length using a sharp cutting tool made of a particular material such as diamond or tungsten carbide and then there is an application of tension in the longitudinal direction to cause the fragile breakeage of the fiber.

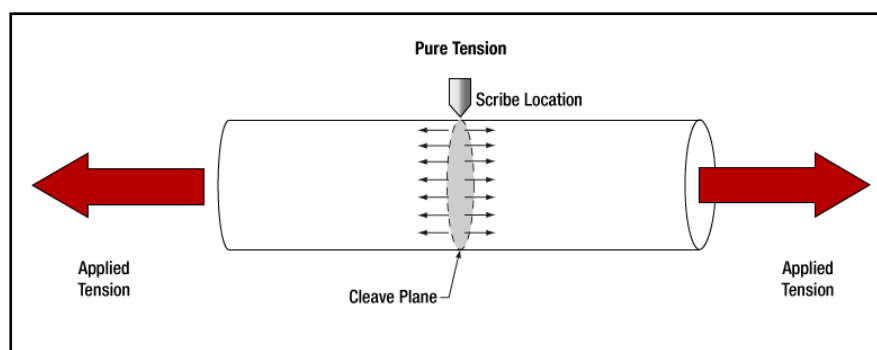


*Figure 22: Representation scheme of cleaving procedure*

In some applications, instead of applying a tensile force, the fiber is bended in the crack area so to cause an excessive tensile stress on the fiber's surface. [25]

To perform cleaving during this work the 'Large Diameter Optical Fiber Cleaver CT 106' made by Fujikura company was used.

This machine applies a clamping force to the fiber and then increase the tension to the desired value in a direction perpendicular to the cleave plane while the fiber's surface get scratched with a very hard diamond edge scribing tools. This make the crack propagates rapidly along the fiber's cross section.

This machine works with particular recipies, made for commercial silica fiber with preset settings values, which were not usable for the Calcium-Phosphate Glass fiber and hollow fiber because of the different mechanical properties. For the samples used during this work different recipies have been created, after different trials, to obtain optimal cleaved surfaces in the samples.

The fiber samples had a cladding diameter of  $150\ \mu\text{m}$  and a core diameter of  $64\ \mu\text{m}$ , and were both end cleaved using the recipie finalized for the calcium phosphate fiber .The first type of cleave was done with the aim to obtain a perfect  $90^\circ$  angle with respect to the longitudinal axis of the fiber. As shown in **Figure 23**, the Fujikura LZM-100  $\text{CO}_2$  laser splicer shows a comparison between the calcium phosphate fiber (left) and a multimode silica fiber (right). The splicer shows an angle of  $0.1^\circ$  for the calcium phosphate fiber and a silica fiber with an angle of  $0.0^\circ$  which was instead cleaved with a Sumitomo FC-8R Precision Handheld Automatic Blade Rotation Cleaver.

The calcium phosphate fiber angle value is pretty fine to obtain a good splice, reducing at the minimum the splice loss with the silica fiber on one end , to observe light guidance from the other end in the characterization of fiber splice and a good splice on both end of the calcium phosphate fiber with the silica fiber for transmission study.

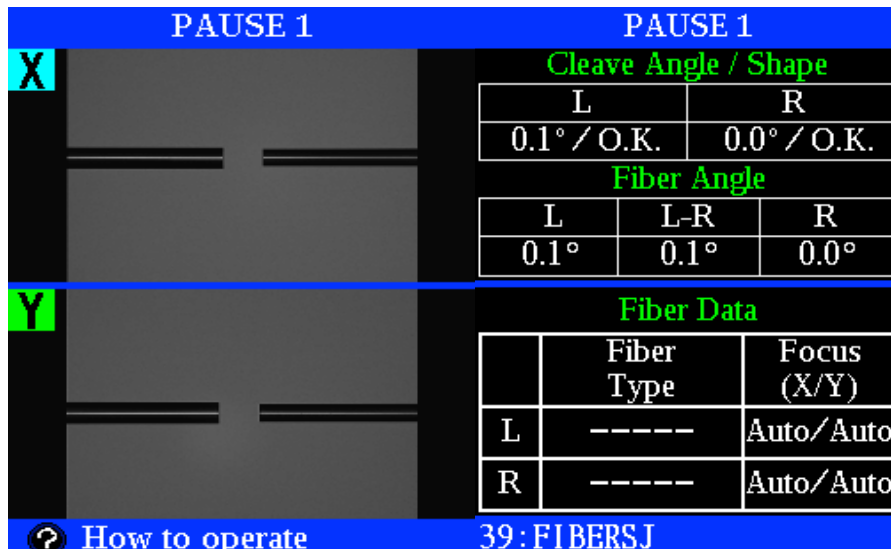


*Figure 23 : Image of the Fujikura LZM-100 CO<sub>2</sub> splicer of the calcium phosphate fiber (left) and the Silica commercial fiber (right)*

The cleaver machine used in this work had also the functionality to perform angled cleaves.

This feature was used to obtain the samples for the angle cut study whose aim was to investigate the dissolution of the fiber tip when this was not perfectly perpendicular to its axis but more sharp and with different angled surfaces.

Angled cleaves were obtained because of a torsion force applied to the fiber by the machine, rotating the right clamp to the predefined rotation angle. The angle values that the machine allows to obtain range from 0 to 15 degrees depending on the rotation angle of the right clamp. In particular, for the angle cut study, the samples were obtained with the same recipe used to get a flat surface, but imposing now a rotation angle for the right clamp of 45°, 60°, and 90° degrees.

In **Figure 24** are shown the cleaved fiber samples obtained by rotating the right clamp of 45° on the left and of 60° on the right, for which the splicer machine calculated an angle value respectively of 12.6° and of 15° degrees.

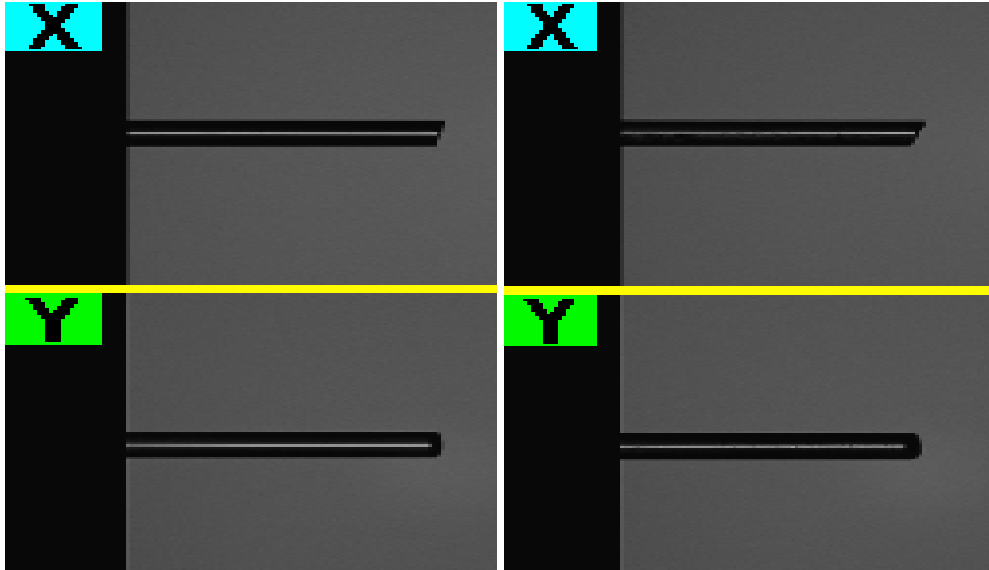


*Figure 24: Images of the Fujikura LZM-100 CO<sub>2</sub> splicer of the calcium phosphate fiber samples obtained with angled cleaves.*

The calcium phosphate hollow fiber has different dimensions with respect to the fiber, so new recipes were made to obtain a surface perfectly perpendicular to the hollow fiber longitudinal axis and surfaces with different angles.

The hollow fiber samples had a diameter of 220  $\mu\text{m}$  and a hole diameter of 110  $\mu\text{m}$ . The first recipe was made defining a clamp force value and a tension value with the aim to obtain a perpendicular angle of cleaving in both end of the sample.

As shown in **Figure 25**, the cleave angle of the hollow fiber on the left is  $1.0^\circ$  and the one of the silica commercial fiber on the right is  $0.9^\circ$ . Still, the value of the angles are acceptable to obtain a quality splice afterwards. Moreover, the laser splicer machine calculates the value of the angles considering also the presence of dust on the samples so before performing cleaving the calcium phosphate fiber, the hollow fiber and the silica fiber were cleaned with isopropyl alcohol. The hollow fiber cleaning with this solution needed more care because of the possibility that the alcohol could penetrates in the hole.

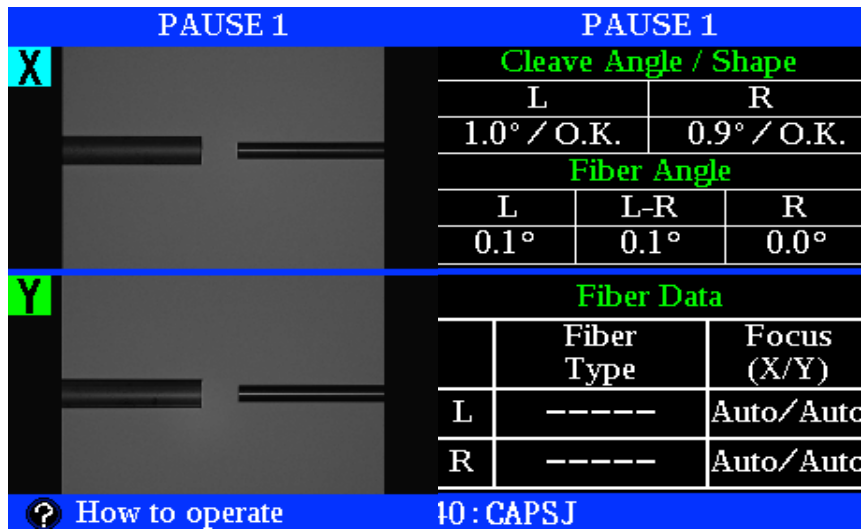


Figure 25: Image of the Fujikura LZW-100 CO<sub>2</sub> splicer of the calcium phosphate hollow fiber (left) and the Silica commercial fiber (right).

Angle cut study was also performed on the calcium phosphate hollow fiber samples, so the same procedure used for fiber samples was again employed to get angled cleaves on hollow fiber samples. The recipe used, to realize these samples for the study, was the one finalized for the calcium phosphate hollow fiber to obtain a flat surface but imposing now a rotation of the right clamp of 45°, 60° and 90° degrees. In the **Figure 26** are show the obtained cleaved angles imposing a rotation of the right clamp of 45° on the left and of 60° on the right.

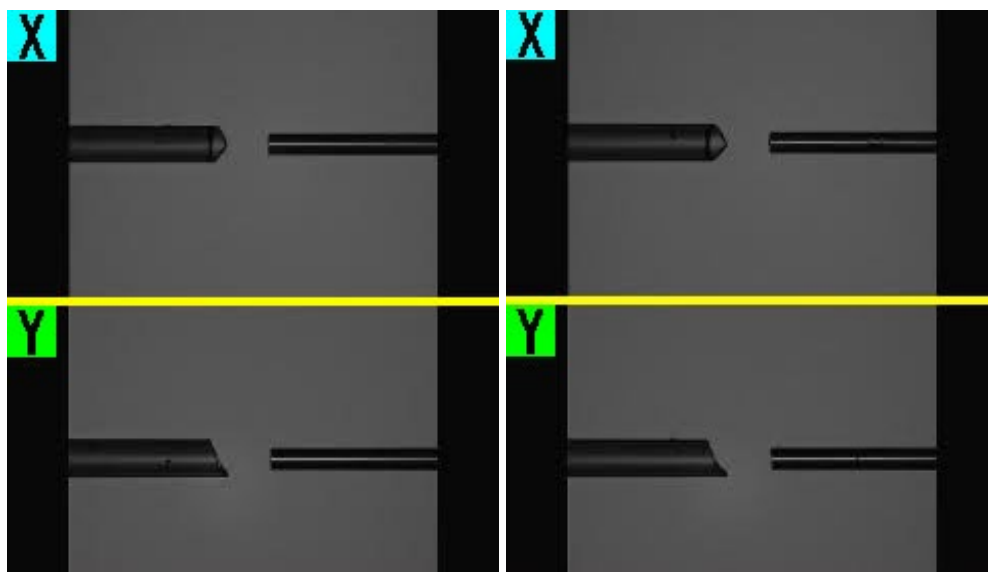


Figure 26: Images of the Fujikura LZW-100 CO<sub>2</sub> splicer of the calcium phosphate hollow fiber samples obtained with angled cleaves.

## SPLICING

The next step, very important for all the studies carried on during this work of thesis, in particular for transmission study, was the splicing of the calcium phosphate fiber and hollow fiber with a commercial multimode silica fiber. As previously said, to study the transmission of light in both the fiber and hollow fiber, the light source was spliced to our samples, so the aim at this point was obtaining a low loss splice and the correct guidance of light.

The splicing process is the common technique employed to realize a joint between two optical fibers. There are two ways to splice optical fibers depending on the insertion loss and performance results. These are fusion splicing and mechanical splicing.

The mechanical splicing consist in aligning the fibers, generally using V-grooves, and keep them in position using epoxy resin or mechanical clips. This type of splice is not permanent and has higher losses than the fusion which perform rather a permanent splice.

The fusion splicing is the method used in this study and consists in joining two fibers together by fusing them electrically or thermally.

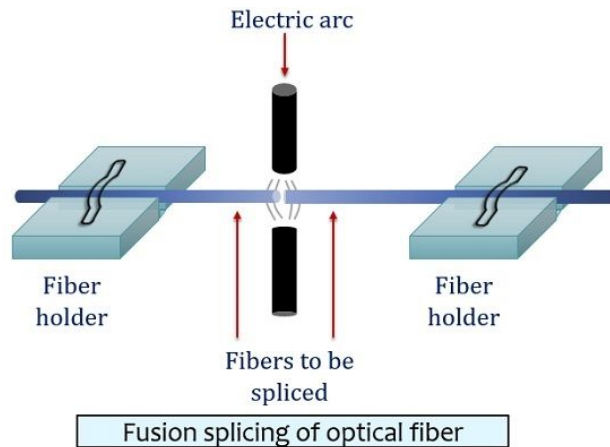


*Figure 27: Example scheme of splicing method using an electric arc to join two fibers [26]*

The aim of the fusion splicing is to fuse the two fibers, when they are aligned in the proper way, so that light can pass through the fibers and is not scattered or reflected at the splice region. The electric arc, which is the most common source of heating used in fusion splicing methods, gives a transparent and non reflective melt region, with low losses.

There are also sources of heat different from the electric arc that can be used to perform melting of the fiber such as laser, gas flame or a tungsten filament. [26]

In this work both electric arc and laser have been used. The first one was used to perform splice between commercial silica fibers while the second was used to splice our calcium phosphate fiber and hollow fiber to a commercial silica fiber. The machine used for splicing the silica fibers was the FSM 40-S Fujikura splicer. The Fujikura LZM-100 CO<sub>2</sub> laser splicer was instead employed to splice the bioresorbable fiber and hollow fiber with the silica fiber and uses a CO<sub>2</sub> laser heat source to heat fibers, eliminating the use of electrode and ensuring repeatable performance. It also very clean because it eliminates any deposits on the fiber surface that could occur by using filament or electrodes. The laser beam from the CO<sub>2</sub> is splitted into two beams to perform an uniform and well controlled heating, obtaining a smooth and contamination-free glass surface. [27]

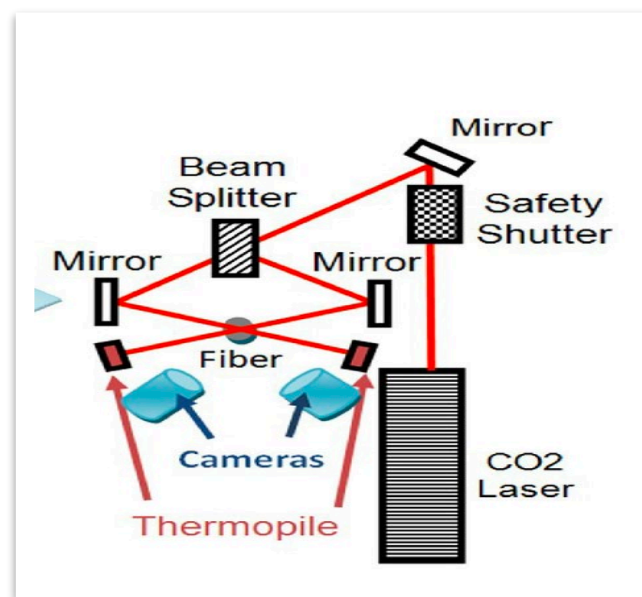


*Figure 28: Scheme of the Fujikura CO<sub>2</sub> laser splicer [27]*

The machine had some particular recipes already set to splice commercial fibers which were used to create other two recipes for our two case of study.

This splice process in particular, was very challenging due to many factors:

- The dimensions of the bioresorbable fiber and hollow fiber samples used were different from the silica commercial fiber dimensions to which both samples were spliced. The silica multimode fiber used in both case has a core diameter of 62.5  $\mu\text{m}$  and a cladding diameter of 125  $\mu\text{m}$ ,
- The composition of the two fiber was different. On one side we have a phosphate glass and on the other a silica one with different properties and most of all, different softening and melting temperatures,

- The mechanical stability of the junction was difficult to achieve as it depends on a combination of many factors such as : the lasing power, the lasing time, the gapset position and the overlap value.

To achieve the best result, the recipe's parameters were adjusted taking into account the factors discussed.

For both case of study, to start the splicing process, the two fibers must be placed in the V-groove clamping system, in order to observe them in the camera. Then, they are brought to a distance defined by the gap parameter that set the distance of the two fiber's facets. The chosen alignment method was the auto one so the two fibers were aligned automatically with respect to the longitudinal axis. A pre-fuse lasing was performed in a short time to increase the viscosity of both glasses and prepare them for the junction. Because of the different softening point between the silica and the calcium phosphate glasses the lasing position was not set at the center of the two fibers but was moved towards the silica fiber. Silica glass has a softening temperature about 1690 °C and melting temperature of 1700 °C while the softening temperatures of the calcium phosphate glass samples used for fiber and hollow fiber fabrication are about 467 °C for the core and 477 °C for cladding and hollow fiber glass while the melting temperature for the calcium phosphate glass is about 500 °C. To reach the softening temperature of silica, the calcium phosphate glass would have been completely melted if the lasing power position wouldn't be moved on silica axis. This gapset position allows to melt enough the silica glass while containing the melt of the phosphate glass.

After melting the two fibers, these undergo a process of stuffing which means they are pushed against each other to increase the mechanical stability of the joint. The amount of stuffing is defined by the overlap and the gap values.

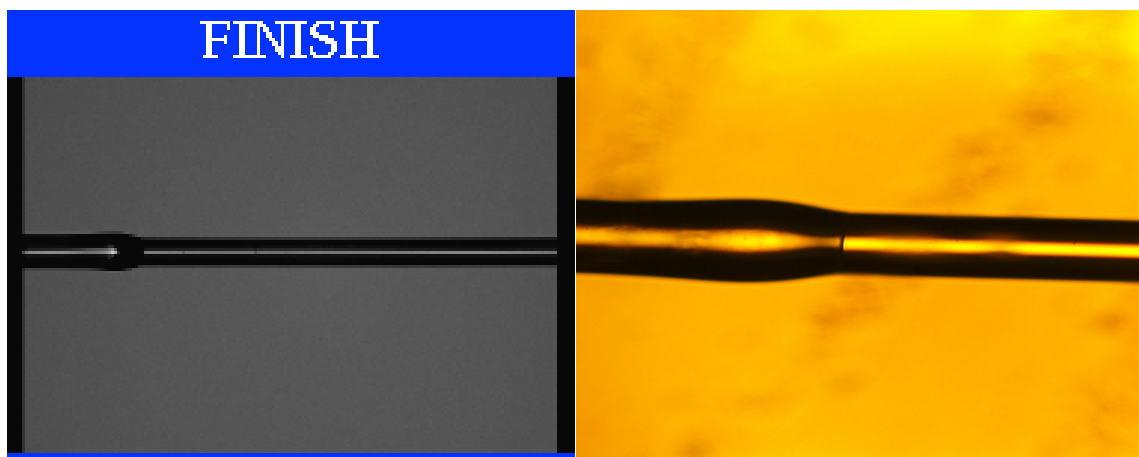


*Figure 29: Image of the result splice between calcium phosphate fiber and silica multimode fiber(left) and the respective optical microscope image(right)*

In **Figure 29** is shown the splice obtained by the ultimate and optimized recipe for the calcium phosphate fiber sample respectively with the CO<sub>2</sub> laser splicer (left) and

optical microscope (right). Fiber splicing recipe was hard to achieve because of its unrepeatability. The most difficult part was finding a good compromise between optical characteristics of the splice region and the mechanical stability of the junction.

After different trials, the final recipe allowed repeatable performances in a lasing time range from 8000 to 8500 ms.

The second case of study, splicing the calcium phosphate hollow fiber with the silica multimode fiber, was performed using the same laser splicer and a new recipe was created.

The main settings were modified because of the different dimensions of the hollow fiber and the overlap increased for mechanical stability, but always taking into account the different glass characteristics, so the process does not change.

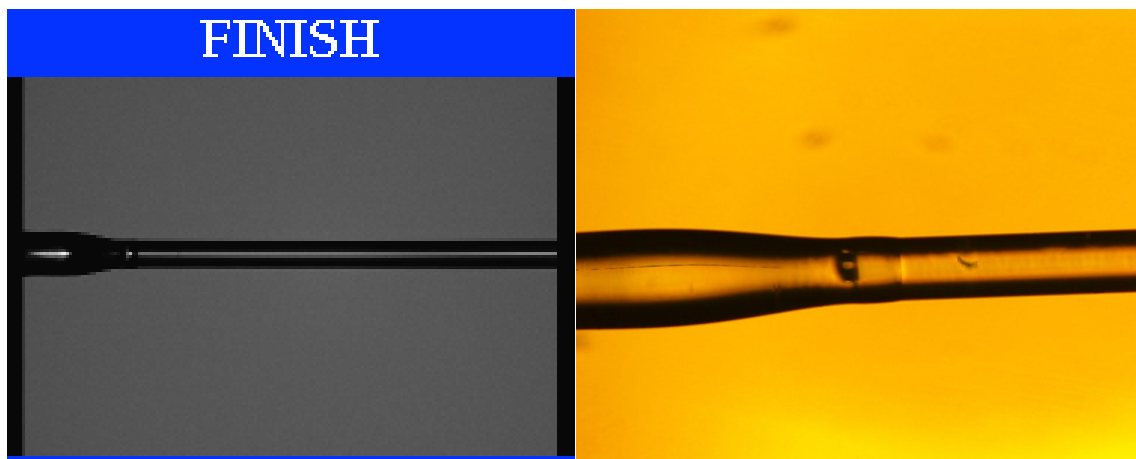


*Figure 30 : Image of the result splice between calcium phosphate hollow fiber and silica multimode fiber (left) and the respective optical microscope image (right)*

The result splice of the calcium phosphate hollow fiber with the silica fiber (**Figure 30**) shows the evident bigger difference in diameter measures of the two fiber with respect to the previous case. Because of this difference, the new splice recipe was made including the tapering functionality.

Tapering is a common technique used on optical fibers to reduce their diameter from few millimeters or centimeters. It is performed stretching the fiber gently after heating, when the glass is still viscous enough to be dilated on the longitudinal axis. This process was also performed to reduce the size of the hole whose presence could disturb the light propagation in the capillary wall by making light propagates inside of it. The recipe created was tested with different samples and optimized to obtain an uniform distribution of light with the maximum of output power and repeatable performances.

## 2.1.2 Characterization of fiber splice

The aim of this study was to splice a multimode silica fiber with the multimode calcium phosphate fiber in one case and with the calcium phosphate hollow fiber in the second case. The light guidance was assessed injecting the light from a laser diode into the silica fiber spliced to the calcium phosphate sample and observing light output from the other sample's end with Xeva XC-130 beam profiling camera using Beam gage software.

The light source employed in this study was the QLM9S470-211 980 nm Laser diode with a maximum output power of 50 mW which is fiber coupled to a single mode silica fiber with a core diameter of 4  $\mu\text{m}$ .

The single mode silica fiber from the laser diode is spliced to a multimode silica fiber with a core diameter of 62.5  $\mu\text{m}$  and a cladding diameter of 125  $\mu\text{m}$ .

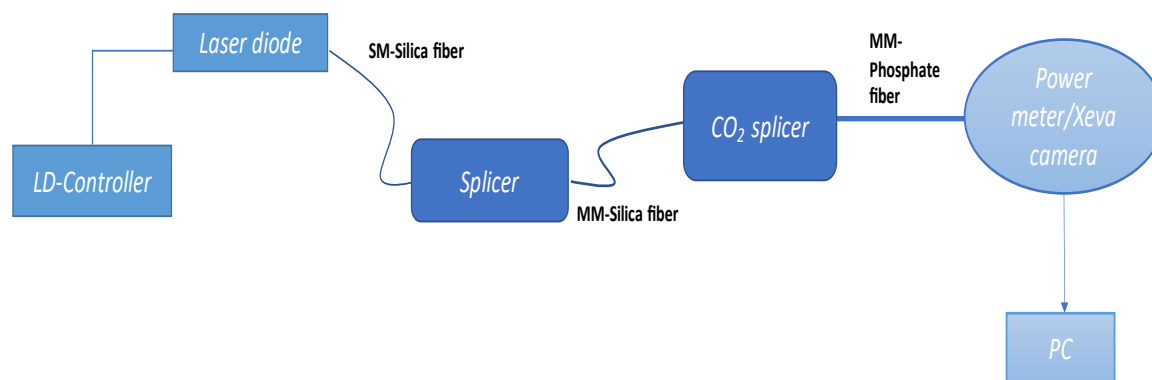


*Figure 31: Experiment setup of preliminary transmission study on phosphate fiber*

As shown in **Figure 31**, the multimode silica fiber was also spliced, through CO<sub>2</sub> splicer, using the recipes finalized for the transmission study in PBS, to the multimode phosphate samples. As previously said, the other end of the samples was cleaved and used to observe light with Xeva camera and to measure the output power using a power meter.

Xeva camera captures and analyzes wavelength in NIR range from 900 to 1700 nm, performing operation at room temperature with a fast data capture rate.

Using a current and temperature controller, the guidance of light was observed at different current values ranging from 25 to 85 mA and maintaining the temperature at 25°C.

Starting from the calcium phosphate fiber, the aim was to confine the light in the core reducing at minimum the presence of light in the cladding.

The splice between the multimode silica and the calcium phosphate fiber was optimized to reduce the phenomena that could cause light escape from the core and the consequent power loss measured at the bioresorbable fiber end.

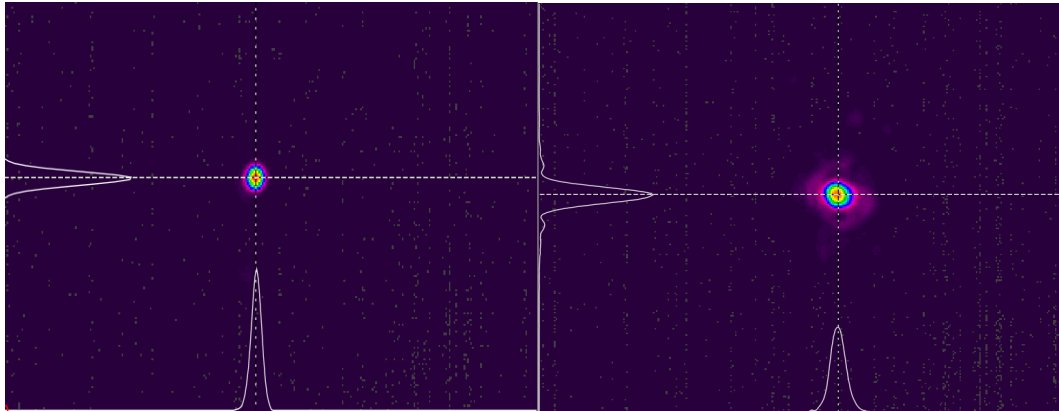


*Figure 32: light captured from the single mode silica fiber (left) and from the multimode silica fiber (right) using Xeva camera.*

In **Figure 32** is shown the guidance of light in the single mode silica fiber on the left and in the multimode silica fiber on the right, captured before the splice between the two fibers.

In camera images is evident the different diameter measure of the cores of the two fibers, where light is well confined.

The multimode silica fiber was later spliced to the multimode calcium phosphate fiber sample of 5 cm of length.

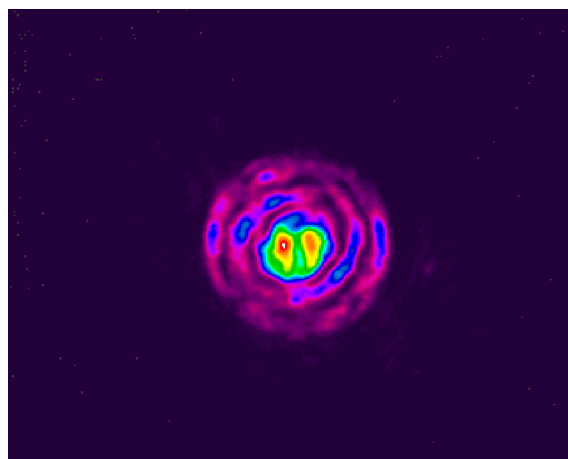


*Figure 33: Light guidance in calcium phosphate fiber core*

In **Figure 33** is shown the final output, coming from the bioresorbable fiber, of light injected with the Infrared laser diode. In the image is visible the light coming from

the core of the fiber, whose cladding is almost totally dark because no light was detected inside of it by camera. This picture was taken to low level of power to not cause saturation of the camera but still to higher power levels, the amount of light in the cladding can be considered negligible with respect to the one present in the core section and this will get probably lost by bending in practical applications. Later, the output power was measured using a power meter. The output power measured with power meter was the sum of the light coming from the core and from cladding.

Different values of current were injected into the fiber so to increase the output power.

The power injected into the bioresorbable fiber was measured at the silica multimode fiber's end, before the splice with the calcium phosphate one, in order to calculate later the total loss caused by the propagation losses of the calcium phosphate fiber and by the splice losses. This power, that will be considered input power, was measured at the output of the silica multimode fiber at the same values of current later tested on the bioresorbable fiber.

Current (mA)	Power IN (mW)
25	7.4
30	10,55
40	16,62
60	29,38
80	41,53
85	44,5

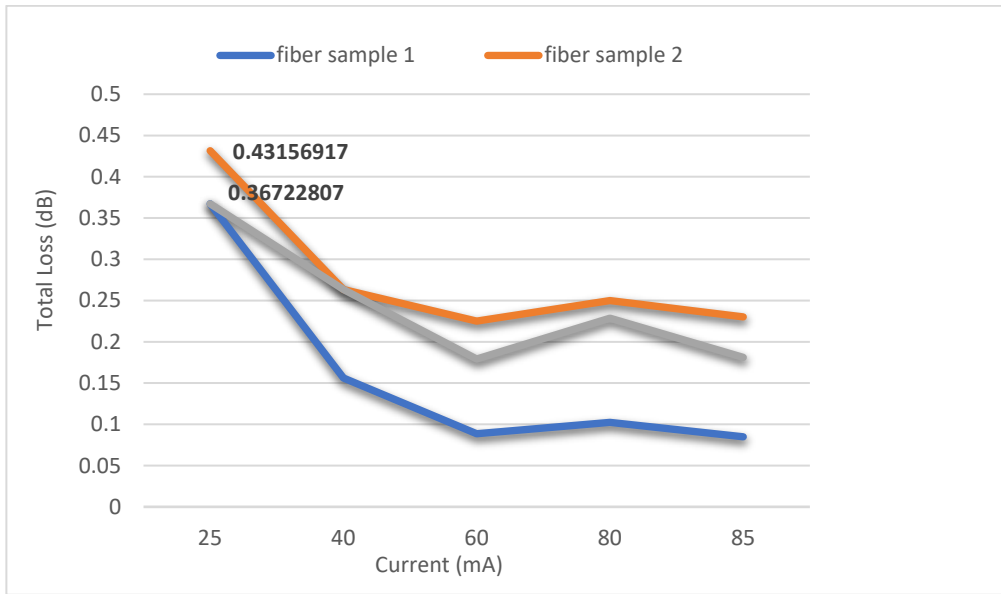
*Table 2: Input power*

The CO<sub>2</sub> splice recipe finalized for this study and for the following transmission study in PBS for the fiber samples was the one capable to reduce the presence of light in cladding but still having a good value of total loss of power.

The total loss was measured on different fiber samples with the same length L of 5 cm under the same conditions with the formula :

$$\text{Total Loss (dB)} = 10 \times \log_{10} \frac{P_L}{P_0} \quad (2.1)$$

$P_L$  is the power coming out from the sample of length L and  $P_0$  is the input power. The total loss does not consider the length of the calcium phosphate fiber because it includes the splice loss which does not depend on the length of the sample but is constant value for a specific spliced sample.



In the graph above is shown the Total Loss calculated for the samples tested with respect to different values of injected current. The total loss shows a decreasing tendency while the current values are increasing and this can be mainly due to more presence of light in the cladding which causes higher values of output power causing an error of underestimate of the total loss. To calculate this value being sure that no light was in cladding, the values of power taken as reference were the ones measured at 25 mA of current because at that level Xeva camera was showing the minimum presence of light in the cladding structure.

The mean value of loss calculated is of 0.4 dB which is a good value for this type of fiber considering it includes the losses caused by the propagation on the 5 cm of length and the splice loss which has a lower value than 0.4 dB.

To better understand the contribution to the total loss of both propagation and splice losses, propagation losses were calculated using a technique called Cut-back. This consists into launching a light power inside a fiber sample and measuring the output power at its end using a power meter. This method implies to start the measurements with a long sample of optical fiber and to progressively reduce its length by cutting it in shorter samples.

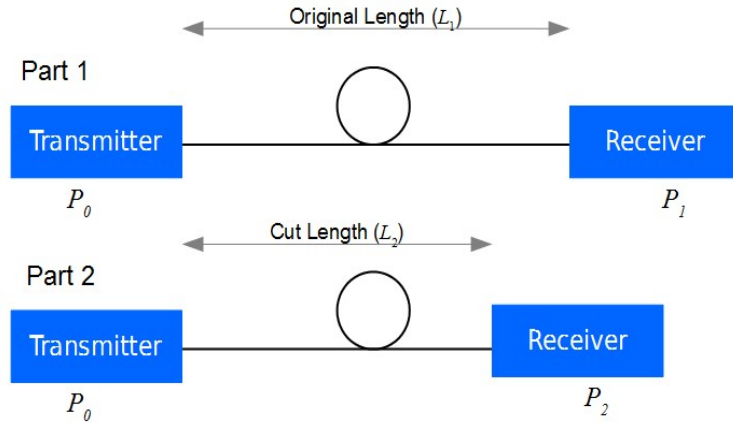


*Figure 34 : Cut-back method scheme*

The result value of loss for the bioresorbable calcium phosphate fiber used in this study was of 2.4 dB/m. This value of loss is reasonable for this type of fiber but still can find further improvements in future by controlling the inhomogeneties in the glass structure, its composition and possible defects at the interface between core and cladding structures. This allows us to conclude that the power lost because of the splice process was simply:

$$\text{Splice Loss (dB)} = \text{Total Loss (dB)} - \text{Propagation Loss} \left( \frac{\text{dB}}{\text{m}} \right) * L(\text{m}) \quad (2.2)$$

Where it is considered that the propagation losses depends on the length  $L$  of sample tested. Obtaining a mean value of splice loss of 0.28 dB for the splice recipe finalized for the calcium phosphate fiber samples used for the next transmission study.

The second part of this study was about the calcium phosphate hollow fiber preliminary transmission study. The experimental setup was the same of the bioresorbable fiber, but this was replace by the hollow fiber so the recipe employed for the splice between the multimode silica fiber and the hollow fiber samples was the one finalized for the hollow fiber transmission study in PBS.

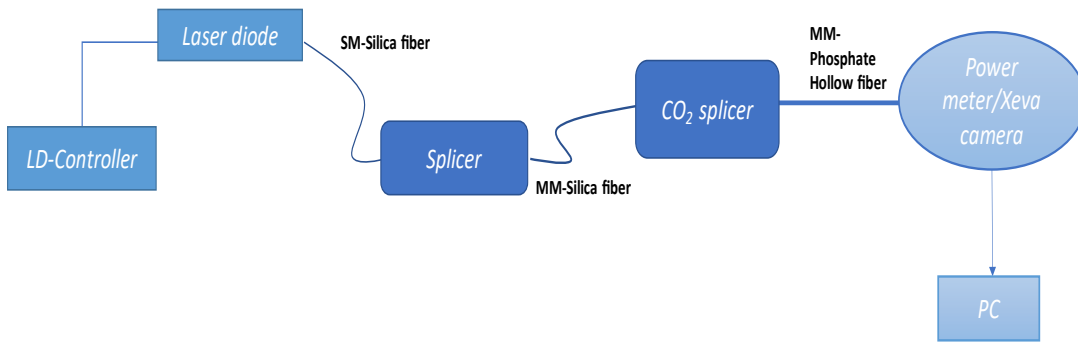


*Figure 35: Experiment setup of preliminary transmission study on phosphate hollow fiber*

The aim of this second case of study was obtaining a good guidance of light in the capillary wall, with the minimum presence of light in the hole, an uniform distribution and low level of splice loss. The trials performed on different samples brought to, as shown in **Figure 36**, an uniform light distribution and no light in the hole section.

The output power measurement trough the cleaved end of the bioresorbable hollow fiber

showed for all the samples tested a maximum value of about 10 mW which means high total losses. For the same input values of power for each value of current shown in the previous table, the total loss calculated for the hollow fiber samples was of 6.2 dB on 5 cm long samples.

These high losses were investigated by changing the splice settings to modify the junction interface between the silica fiber and the calcium phosphate hollow fiber trying to reduce the power lost at the splice point.

The propagation losses calculated trough the cut back method demonstrated that the most of the losses calculated were caused by intrinsic parameters and not because of splice process.

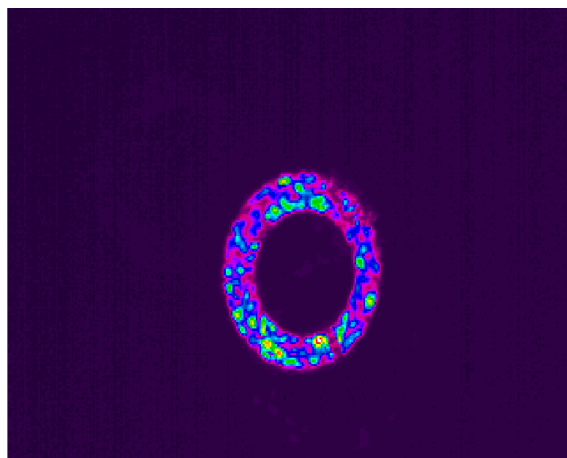


*Figure 36: Light guidance in calcium phosphate hollow fiber wall*

## 2.2 Fiber and hollow fiber behaviour in PBS solution

Phosphate buffered saline or PBS is a buffer solution commonly employed in biological research. Buffer solutions are aqueous solutions capable of keeping the pH value almost constant when a small quantity of acid or base is added. It consists in a solution of weak acid and its conjugate base or vice versa. The pH adjustment is achieved by releasing protons when they are consumed during a reaction or reducing their number when they are released in a reaction. This type of solution can work until a limit is reached, after its maximum capacity the solution will no longer act as buffer with the consequent easy changing of the pH value. PBS is a buffer mainly made of water and salt containing disodium hydrogen phosphate, sodium chloride, potassium chloride and potassium dihydrogen phosphate.

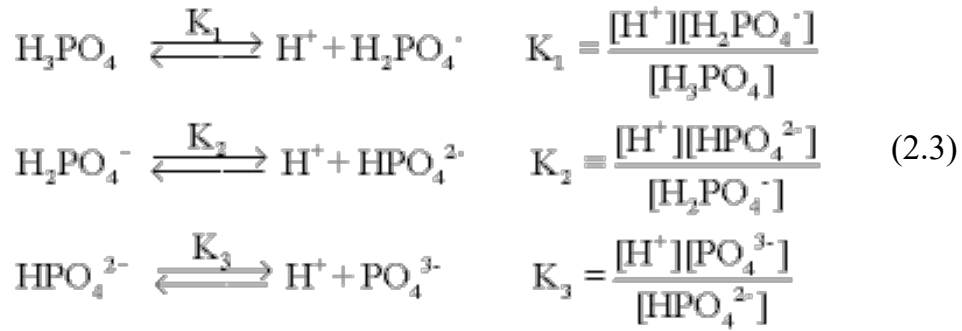
This solution at pH value of 7.4 is mostly used because it mimics the ion concentrations, osmolarity and pH of the human body. When PBS solution is in contact with cells or blood the isotonicity of the solution won't lead to any concentration gradient that causes diffusion of water molecules across the cell membrane. [28]

For these reasons, PBS solution was chosen as means to test calcium phosphate fiber and hollow fiber behaviour in a simulated biological environment.

The main focus of this section will be the study of the degradation aspects of the bioresorbable fibers in biological conditions, examining the possible risks of their applications on a human body and their ability to maintain stable functionalities while degrading in one month inside the body. For all the tests that will be discussed in this subchapter a PBS solution 1X at a pH of 7.4 will be used maintaining its temperature constant at 37 °C.

The preparation of the PBS solution employed started from a 10X PBS stock solution with a pH of 7.4 at 37 °C. To accurately obtain the final 1X concentration this was diluted with Milli-Q water so to have the 90% of water and the 10% of PBS 10X. After dilution the pH was measured with a pH meter to be sure that there was no change in its value. The measurement showed an increased value of pH to 8 which was brought back to its previous value using a 1mM solution of HCl. To calculate how much HCl was needed to adjust the pH, different aspects of the buffer solution were considered, creating a system of equations that were solved to determine the species, whose quantity was actually effecting the pH value.

PBS contains the orthophosphoric acid which undergoes a three ionization steps which can be expressed by their equilibrium constants. These describe the relation between the products and the reactants of a reaction and their values are known.



After these equations, we need to consider the equation of mass balance and we decide to do it on the phosphate. The concentration of the phosphate does not change no matter all the process of dissociation involved.

This equation relate the concentration at the equilibrium of the species to the analytical concentration of the different solutes.

These equations are not enough to solve the system of unknowns so we need to add the equation of balance of charge and the formula of the pH.

The balance of charge is based on the assumption that electrolytic solutions are neutral.

In this case, the concentration of the positive charge is always equal to the negative charge concentration.

The pH value is defined as the negative logarithm in 10 base of the molar concentration of the ions  $H^+$

$$pH = -\log_{10}[H^+] \tag{2.4}$$

Considering that we know the desired value of the solution pH which is 7.4 we calculate the concentration of ions  $H^+$ .

After doing the reasonable approximations we can solve the system of 5 equation and 5 unknowns with a Matlab program. [29]

## 2.2.1 Dissolution test

The dissolution test is a common characterization method for testing the biocompatibility and the degradation rate of a material.

In this work, the dissolution test was performed on both samples of calcium phosphate fiber and hollow fiber. The samples prepared for both type of fiber had a length of 2 cm and were soaked in PBS solution for 30 days keeping the temperature constant at 37 °C.

The aim of this study was observing diameter reduction of the samples at different time steps which were 3,7,14,21 and 30 days. The samples diameters were measured

before soaking them in the solution and showed a value respectively for the fiber and for the hollow fiber of  $150 \pm 3 \mu\text{m}$  and of  $220 \pm 3 \mu\text{m}$ .

For each time point, three samples were removed from a container and dried before diameter measurement. For each of the three samples, at least 15 measurements of the diameter were taken on its length using Optical Microscope. The mean size and the standard deviation of the measurements were calculated for each time points.

A refresh of the PBS solution where the samples were soaked was performed twice a week to mimic the human fluid exchange.

Six containers, where at least four fiber were soaked, have been used so to have a different container for each day of measure. Each container was filled with 4 ml of PBS solution.

For this test the solution volume/samples exposed area was of  $0.10 \text{ ml mm}^{-2}$ .

The same procedure was applied for the hollow fiber samples but with a solution volume/samples exposed area of  $0.07 \text{ ml mm}^{-2}$ . To avoid PBS evaporation the containers were close with parafilms.

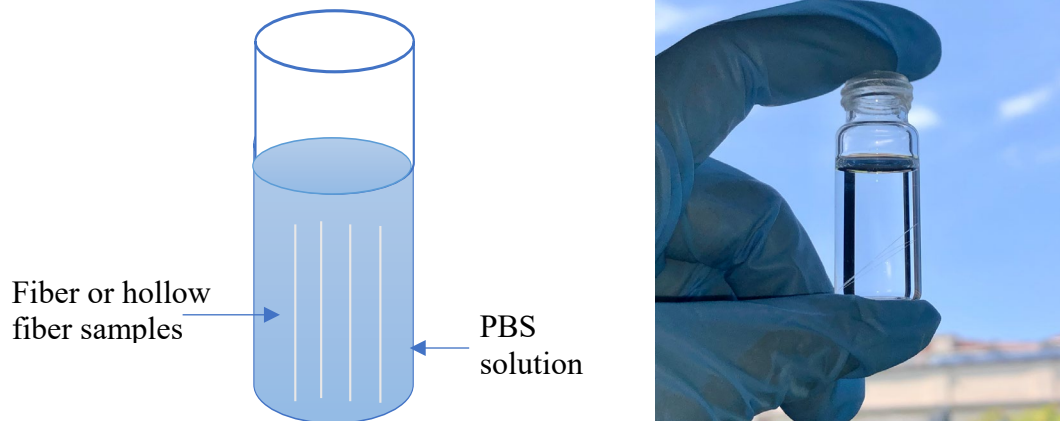


*Figure 37: Dissolution test setup*

## **2.2.2 Angle Cut**

The angle cut study was performed to investigate the dissolution of the tips of both calcium phosphate fiber and hollow fiber. The aim of this study was to observe how sharp edge of both fibers could change their shape while degrading inside the body simulated, in our case, by PBS solution.

Biological applications can experience fiber breakage while handling it inside the body near to soft tissues and organs. The greatest risk is the possibility that a breakage that causes a sharp edge to the fiber can cause wounds in the surrounding tissues.

In this way, the fiber before being metabolized and removed through erosion and enzymatic degradation processes, can bring to several damages to the body.

The analysis started with the preparation of both fiber and hollow fiber samples that were cleaved using the cleaver machine feature to realize angled cleaved as described in **chapter 2.1.1**.

For both type of fiber three samples were realized, imposing to the cleaver machine a rotation of the right clamp of 45, 60 and 90 degrees. The angled tip were later observed with the optical microscope and the size of the angles were estimated making a mean of three different measurements.



*Figure 38: pictures taken with the optical microscope of fiber (left) and hollow fiber (right) samples cleaved by imposing a rotation of 45° to the right clamp.*

The experiment foresaw to keep the tips of the samples soaked in the PBS solution and to measure the change of the angles every three days.

For angle measurements, the sharpest angled side of the sample was chosen as reference, hence the need to keep the sample always stack in the same configuration, while soaked, brought to the realization of a 3D printed model of a particular cap for a laboratory bottle.

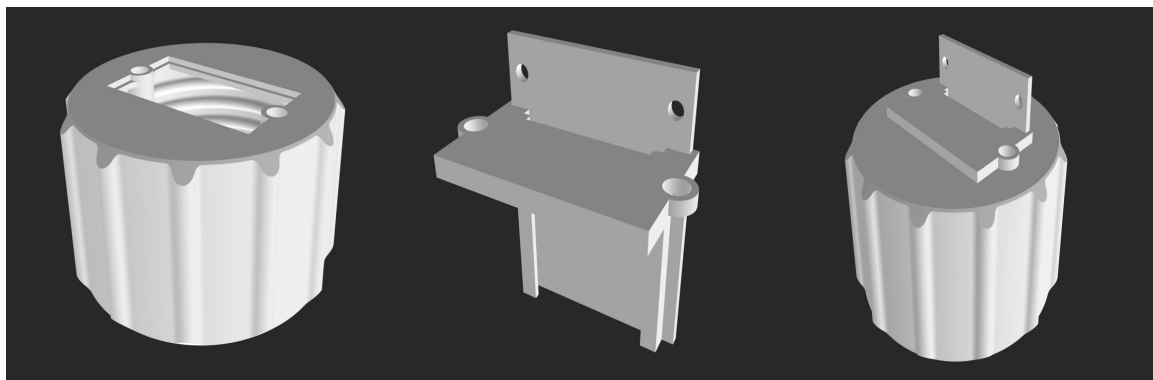


*Figure 39: 3D model of laboratory bottle's cap*

The print was made using a Stratasys uPrint SE available in DIMEAS department in Politecnico di Torino. This 3D printer uses a Fused Model Deposition (FDM) technology to realize accurate models in ABSplus thermoplastics. The FDM is an additive manufacturing process that builds objects layer by layer by selectively depositing melted material and using thermoplastic polymers in the form of filament.

The cap of the bottle was designed to include an easy removable piece where a blank glass slide for optical microscope could run. This piece was designed considering the dimension of the slide and the diameter of the bottle where it was inserted. The slide was used to keep the fibers in the same configuration by blocking them with glue after choosing the fiber side of interest. Two holes in the cap were designed with the aim to install threaded brass inserts to ensure a joint between the cap and the removable piece, which was also designed with two inserts for the screws. The holes in the cap were designed to have smaller dimensions compared to the inserts to take into account any plastic melt when installing them. Using a soldering iron to heat for 3 minutes the plastic it was possible to install the inserts perfectly. All this was made to guarantee both static conditions during the study, with no perturbation of the fiber samples, and an easy removal of the slide when measurements had to be taken.

Two identical caps were printed for the angle cut study respectively of the calcium phosphate fibers and the hollow fibers.

For angle cut study of the fiber tips the solution volume/samples exposed area was of  $5,30 \text{ ml mm}^{-2}$  while for the study of hollow fiber tips it was  $3,61 \text{ ml mm}^{-2}$ .

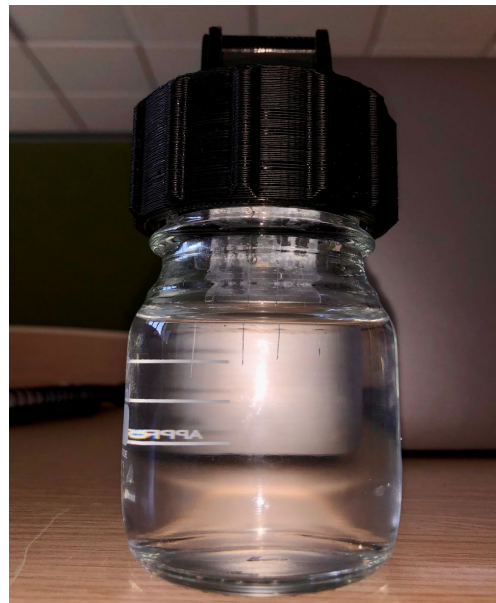


*Figure 40: Angle cut study setup using the 3D printed cap to suspend the slide where the samples are attached, soaking their tips in PBS*

## 2.2.3 Transmission study

The transmission study was conducted on a calcium phosphate fiber sample to evaluate how the optical characteristics of this type of fiber, which were deepened in the characterization of fiber splice study, faced up in **chapter 2.1.2**, could be affected by a simulated biological environment in a 30 days experiment.

A 12 cm long fiber sample was cleaved on both end to obtain flat surfaces for the following splice to multimode silica fibers on both ends. The aim was to keep soaked in PBS solution the phosphate fiber, while the silica remain outside of the container for the other connections, and observe how the degradation of the fiber would effect light's propagation.

The splice between the silica fibers and calcium phosphate fiber was obtained using CO<sub>2</sub> splicer as described in **chapter 2.1.1**.

To protect the joint between silica and phosphate fiber from any stress and prevent breakage, fiber optic thermal sleeves have been employed. The sleeve inner tube is made of ethylene vinyl acetate (EVA) material and the outer one of polyolefin. The sleeve has inside a stainless steel rod for mechanical stability, when the sleeve is heated it shrinks holding tightly the rod to exclude air. The sleeves have been heated using the Fujikura fusion splicer shrink oven to guarantee a complete protection of the glass fiber in the splice points.

In **Figure 41** is shown the schematic configuration of this study. The calcium phosphate fiber was soaked in PBS solution inside of a container keeping its temperature constant at 37°.

The container was filled with almost 200 mL of PBS and no refresh of the medium was performed during the test period to not perturb the system, with the high risk to break the fiber, and because of great volume of solution employed.

The fiber was fixed in the same configuration using hot glue to hold the fiber tightly to the container at the thermal sleeves sections, on both side. The silica multimode fibers already spliced to the phosphate one were used, in one end, to inject light through all the fiber and, in the other end, to measure the output power level using a power meter.

The light source employed for this study was the same used for the characterization of fiber splice study, the QLM9S470-211 980 nm Laser diode fiber coupled to a single mode silica fiber with a core diameter of 4 μm.

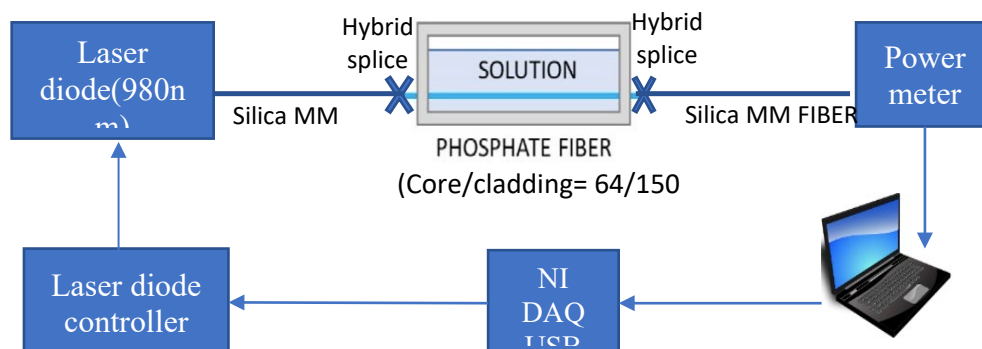


*Figure 41: Transmission study experimental setup*

The first silica multimode fiber was spliced from the free end to the single mode fiber of the laser diode using Fujikura splicer and light injection was possible thanks to a Newport Laser diode controller.

The output power was measured from the free end of the second silica multimode fiber using Thorlabs PM16-121 - USB Power Meter with a standard photodiode sensor.

The power injection was automatized using the remote control function of the laser diode controller combined with the Instrument Control Toolbox of MATLAB. The toolbox allows to connect instruments via instrument drivers such as IVI and plug&play using the common communication protocols such as GPIB, VISA, TCP or UDP.

The laser diode controller was connected using a GPIB-USB cable to the computer and it was installed thanks to NI MAX software and to all the NI drivers as NI-VISA, NI-DAQmx and NI 488.2 that were needed to provide the access to the hardware.

With the instrument control toolbox it was possible to write a matlab program to send out to the laser diode controller, specific commands, in our case, the commands to switch the current on, set the value of the desired current and switch off again. The temperature control was set to 25° for all the time. The program was written to send these commands once every hour for two particular values of current which were 80 and 100 mA.

The respective output power for these values of input current was recorded using the Thorlabs power meter's software, Optical Power Monitor.

This software allows to acquire measurement statistics over a set time or data sample size and to export all data in .csv format.

The recorded data, exported in multiple csv files, were later processed to calculate a mean value of power for each day of recording for each value of input current.

At the end of the study the pH value of the PBS solution where the calcium phosphate fiber remained soaked was measured to evaluate any change in its value. After light transmission interruption the fiber was observed with optical microscope to investigate the dissolution status and diameter measurement was taken.

For transmission study the volume of solution /sample exposed area was of 3.53 ml mm<sup>-2</sup>.



## 3. Results

In this chapter, the results obtained from the different studies carried on during this work of thesis will be presented.

The aim of this section will be to analyze these results by focusing on the biological processes involved in all the experiments, in which the calcium phosphate fibers and hollow fibers were in contact with a solution that was chosen to mimic the physiological environment of the human body.

Moreover, the optical characteristics and the maintenance of the optical fiber's functionality in this type of environment will be explored and deeply discussed.

### *3.1 Dissolution test*

The dissolution test performed on the calcium phosphate fiber and hollow fiber allowed us to study the dissolution kinetics of these type of glass and their solubility in PBS solution.

The PBS solution pH was not evaluated during this test since it has already been done in a previous study for the same glasses compositions and it was assessed that its value remained in physiological range from 7.2 to 7.4 for both type of glasses employed in this study.

The degradation of calcium phosphate based glasses strictly depends on the glass composition. In fact, it was already demonstrated that the more content of MgO oxide in the glass composition the slower dissolution rate. This implies that MgO increases the stability of the glass network more than the CaO. As already said the  $Mg^{2+}$  ion as a smaller ionic radius than  $Ca^{2+}$  so is capable of creating stronger bond between non-bridging oxygens of two chains.

These glasses dissolve in aqueous media by reacting with the  $H_2O$  molecules and the ionic species of the Phosphate Buffered Saline solution (PBS) breaking the P-O-P bondings.

As first, the phosphate glass ions react with the species present in the solution to form solid species and hydration reactions take place to form hydroxides.

Second, there is the surface dissolution of these species, where the phosphates are dissolved through hydrolysis process. The dissolution depends on many factor as pH, temperature of the solution and the different ion concentration. While the glass dissolve the ions concentration of the solution change, it get saturated and can form precipitate like hydroxyapatite on the fiber surface. [30] [31]

For both calcium phosphate fiber and hollow fiber the dissolution was observed with optical microscope and for each time step diameter measurement and picture of the fiber will be reported.

The test for both fiber was carried out following the procedure described in **chapter 2.2.1**.

## CALCIUM PHOSPHATE FIBER RESULTS

The fiber samples tested had a diameter of  $150 \pm 3 \mu\text{m}$  on the 0 day before soaking them in the solution.

In **Figure 42** is shown the diameter changing measured with optical microscope for each day of measure. For all the diameter measurements, taken on each day for three different samples, the mean was calculated with the respective standard deviation.

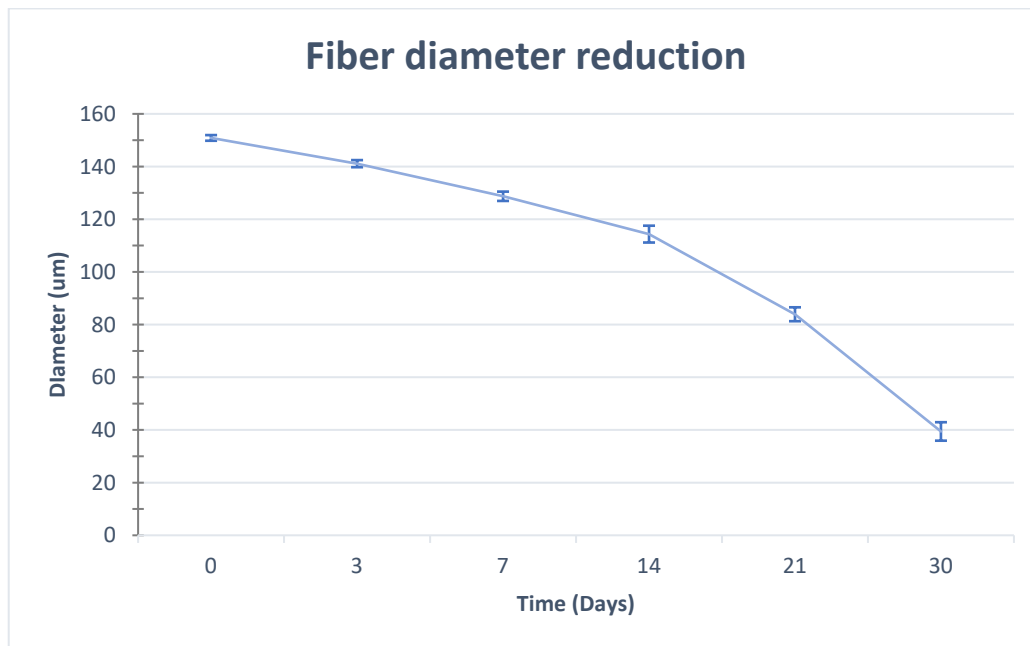


*Figure 42 : Diameter changing of the fiber samples over the time of immersion in PBS solution.*

The fiber samples was composed by two type of glass with a different composition of MgO and CaO. It showed a reduction of diameter almost linear for the first two weeks and then a strong reduction for the last two weeks achiving a diameter value of  $39,42 \mu\text{m}$ . This different rate of dissolution can be explained considering the glass composition of the fiber core and cladding. The first type of glass exposed to the PBS is the cladding one, whose composition has an higher value of MgO. As already said, magnesium oxide works as enhancer of the glass network and this is why for the first two weeks the dissolution and so the diameter reduction of the fiber is contained. The core glass, protected by the cladding one is not exposed to PBS initially. This glass composition has a low content of MgO and higher content of CaO. It is presumable to assume that as the fiber degrades, not always in an uniform way, and core glass is exposed to the solution, the dissolution rate increases because of decrease in the glass composition of MgO. The dissolution rate in diameter, for the first two weeks, is about  $2\text{-}3 \mu\text{m day}^{-1}$  but it increases drastically in the last two weeks achiving a value of  $4\text{-}5 \mu\text{m day}^{-1}$ .

In **Figure 43** are showed the images taken with optical microscope of the diameter reduction for each time step. Also from the pictures is evident as for the first two weeks the fiber diameter reduction is not so strong as for the last two weeks when the diameter has rough fall.

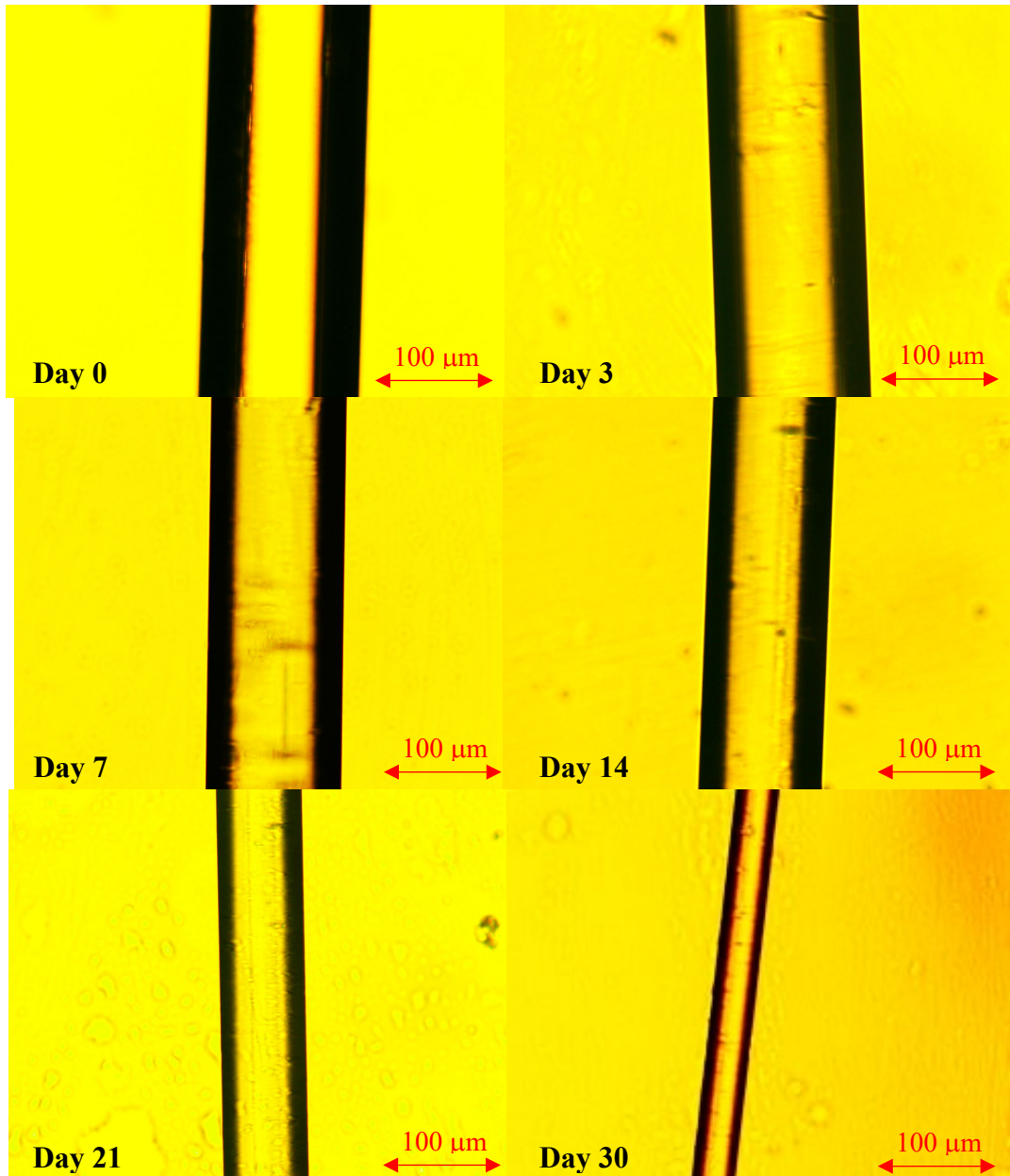


*Figure 43 : Fiber samples picture taken with optical microscope over the days of dissolution showing the diameter reduction of the fiber in PBS solution*

## CALCIUM PHOSPHATE HOLLOW FIBER RESULTS

The calcium phosphate hollow fiber samples had a diameter of  $220 \pm 3 \mu\text{m}$  on day 0 before soaking them in PBS solution.

The hollow fiber study was interrupted before the fiber study because the dissolution was faster for this type of fiber structure. In **Figure 44** is shown the diameter reduction of the calcium phosphate capillary over the days of immersion. From all the diameter measurement for each day, also in this case, it was calculated the mean diameter, for three different samples, and the respective standard deviation value.

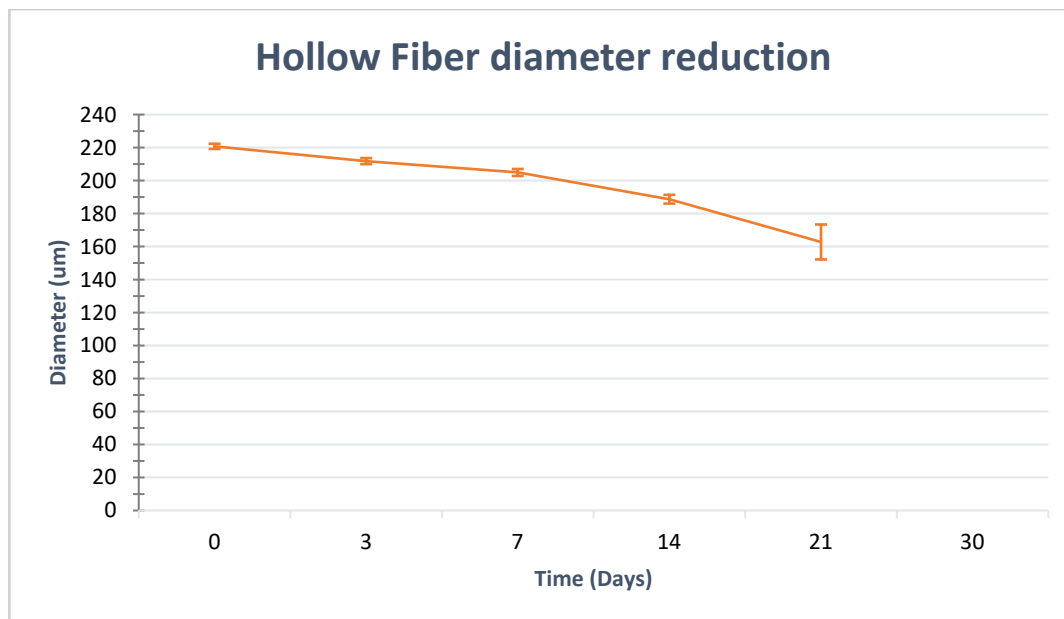


*Figure 44 : Diameter changing of the fiber samples over the time of immersion in PBS solution*

Since the hollow fiber glass had the same composition of the cladding glass of the fiber samples, the external diameter reduction is in percentage similar to the fiber one. There is, in fact, a reduction of much or less  $15\text{-}20 \mu\text{m}$  per week for both hollow fiber and the fiber in the first two weeks before the core glass exposure to the solution. The hollow fiber, differently from the fiber, has a hole inside its structure where the solution can penetrate.

This structural aspect makes the hollow fiber dissolve faster because it degrades both from the outside and from the inside.

The hollow fiber wall thickness is  $55 \mu\text{m}$  because the hole has a diameter size of  $110 \mu\text{m}$ . From an estimate, degrading from both side of almost  $20 \mu\text{m}$  per week it means that the hollow fiber will be completely dissolved after the 21<sup>th</sup> day of immersion in PBS solution. As shown in the graph in **Figure 44** no diameter measurement were taken after the 21<sup>th</sup> day because no hollow fibers have been found in the container at the 30<sup>th</sup> day as they were already dissolved.

The hollow fiber samples were not visible in the container starting from the 26<sup>th</sup> of immersion in the solution. The dissolution rate in diameter, was of almost  $3 \mu\text{m day}^{-1}$ . From the pictures of **Figure 45**, showing the diameter reduction of the calcium phosphate hollow fiber samples, is visible how in the last day of diameter measurement, the wall thickness of the sample is just a few micrometers.

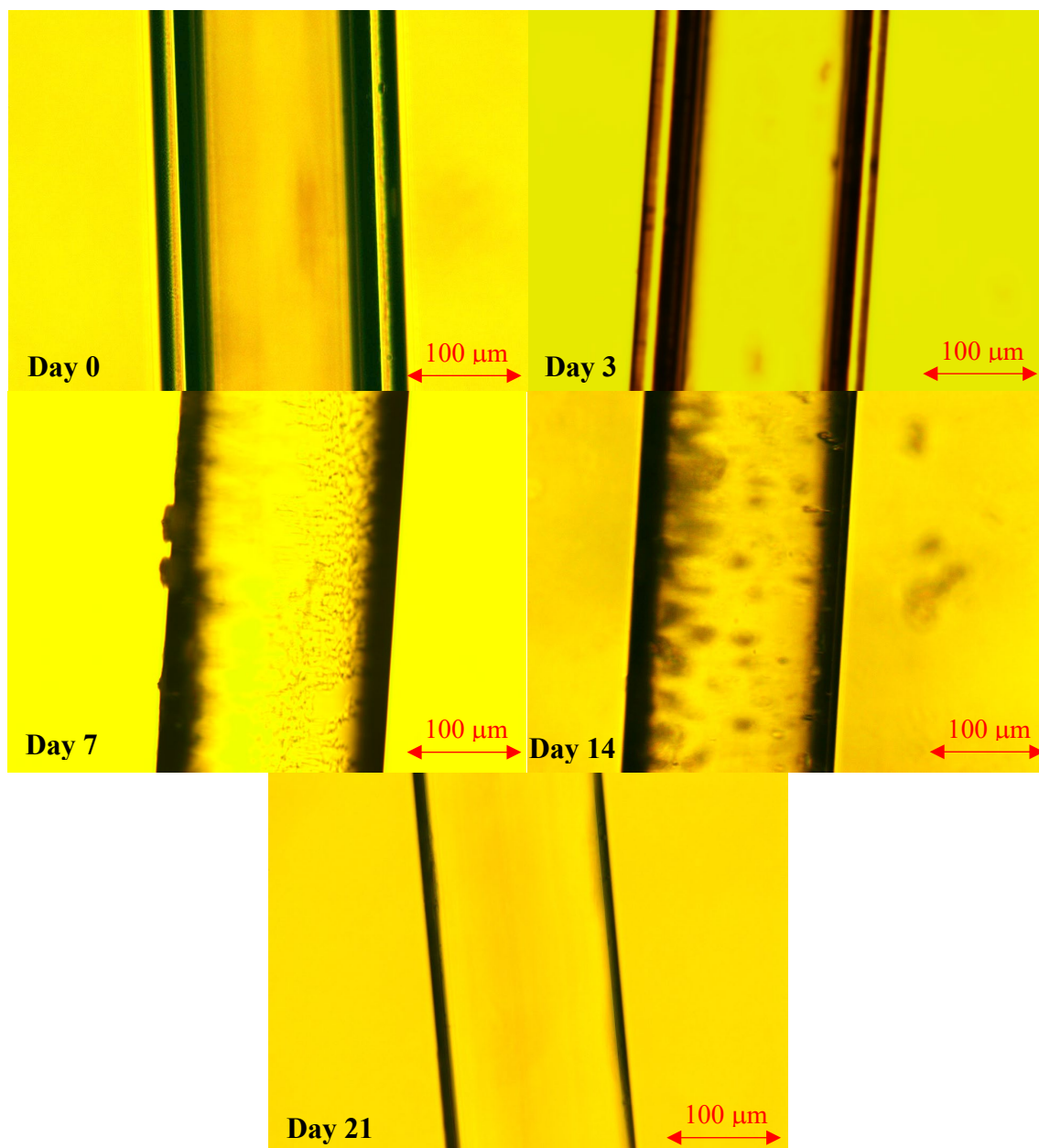


*Figure 45 : Hollow Fiber samples picture taken with optical microscope over the days of dissolution showing the diameter reduction of the hollow fiber in PBS solution*

Further studies for dissolution tests on the calcium phosphate fibers could investigate the growth of bacteria on the fiber surface like also the formation of hydroxyapatite layer while soaked in PBS. Another further study could be to redo

this test in Simulated Body Fluid (SBF) which is a solution that has ions concentration similar to that of the human blood plasma.

This solution is commonly employed to study the bioactivity of glass ceramic, in particular, to study the bone bioactivity where the formation of apatite layer on the glass surface is really important.

This solution was not chosen for this study because the final intended use of the calcium phosphate fiber is not to be implanted in bone tissues.

### 3.2 Angle cut

The angle cut study was performed on both calcium phosphate fibers and hollow fibers to observe how sharp edge, realized on these fibers, could change their profile soaked in PBS solution, while degrading. The test was conducted following the procedure described in **chapter 2.2.2**.

The expected results were to see the tips of the fiber samples become rounded in a few days from the immersion in PBS solution. While the ions get released in the solution and solid particles of the material are removed causing the dissolution of the glass, the sharp tips of the fibers should loose material reducing their sharpness. The test was carried out for 20 days and it was interrupted because the fiber diameter got strongly reduced from day 16 to 20 that it was completely dissolved on the 24<sup>th</sup> day.

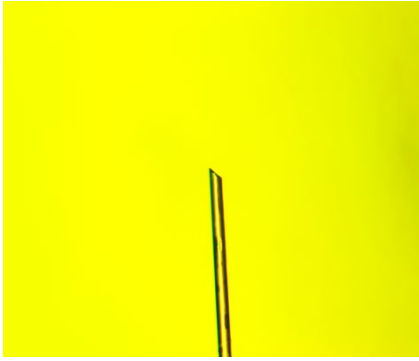
Since the volume of solution/area of the samples exposed was different for this study respect to the dissolution test performed, we have also evaluated the diameter reduction in relation with the angle size. A graph for each fiber will be reported.

#### CALCIUM PHOSPHATE FIBER ANGLE CUT STUDY RESULTS

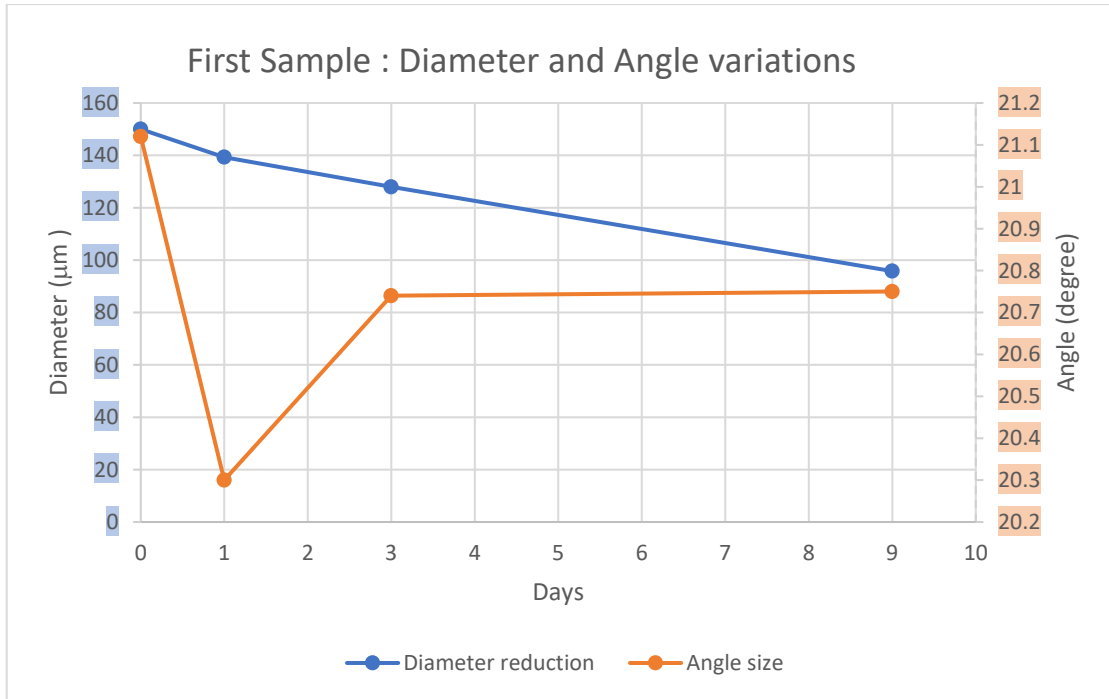
The first results that will be presented are the ones for the fiber cleaved with a rotation angle of the cleaver machine's right clamp of **45 degrees**.

<i>Days of immersion</i>	<b>Day 0</b>	<b>Day 1</b>
<i>Pictures of fibers tips</i>		
<i>Angle size</i>	21,12°	20,3°

<i>Days of immersion</i>	<b>Day 3</b>	<b>Day 9</b>
<i>Pictures taken with optical microscope</i>		
<i>Angle size</i>	20,74°	20,75°

<i>Days of immersion</i>	<b>Day 16</b>	<b>Day 20</b>
<i>Pictures taken with optical microscope</i>		
<i>Angle size</i>	//	//

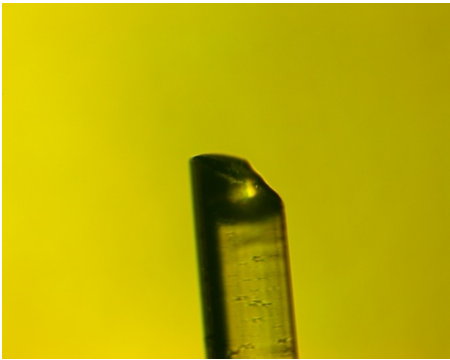
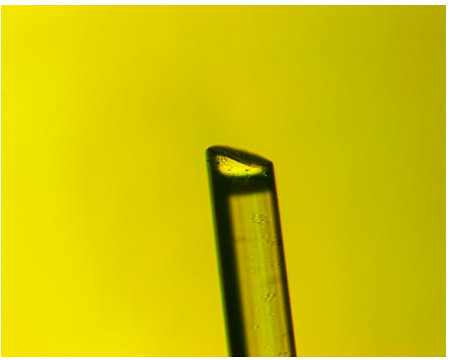
The fiber sample changing were not so remarkable until the 16<sup>th</sup> day, nevertheless the care in handling the samples , the fiber sample showed a breakage on one side possibly because of a crack that was actually visible on the third day of measure. There was no meaning in measuring the angles size for the following days because they were not a result of the erosion of the tips but of an accidental crash while removing the sample from the container or when placing it on the glass slide to be observed with optical microscope. The size of the angle remained almost constant for all the days of immersion.

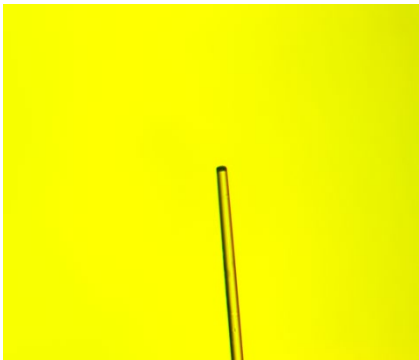


*Figure 46: Plot of diameter and angle reduction in a volume of 100 mL of PBS*

The second fiber sample was instead obtained by imposing a rotation of the right clamp of the cleaver of **60 degrees**:

<i>Days of immersion</i>	<b>Day 0</b>	<b>Day 3</b>
<i>Pictures of fibers tips</i>		
<i>Angle size</i>	31,56°	35,73°

<i>Days of immersion</i>	<b>Day 9</b>	<b>Day 13</b>
<i>Pictures of fibers tips</i>		
<i>Angle size</i>	47,95°	30,79°

<i>Days of immersion</i>	<b>Day 16</b>	<b>Day 20</b>
<i>Pictures of fibers tips</i>		
<i>Angle size</i>	34,4°	31,4°

The second sample didn't show great changes in shape and angle size until day 9 when part of its tip became flatter which was auspicious. On day 16 the tip became a little sharp again but its diameter was so small that it is very unlikely that could cause injuries inside the body. On day 20 the tip was almost completely flat and the fiber diameter was about 10  $\mu\text{m}$ .

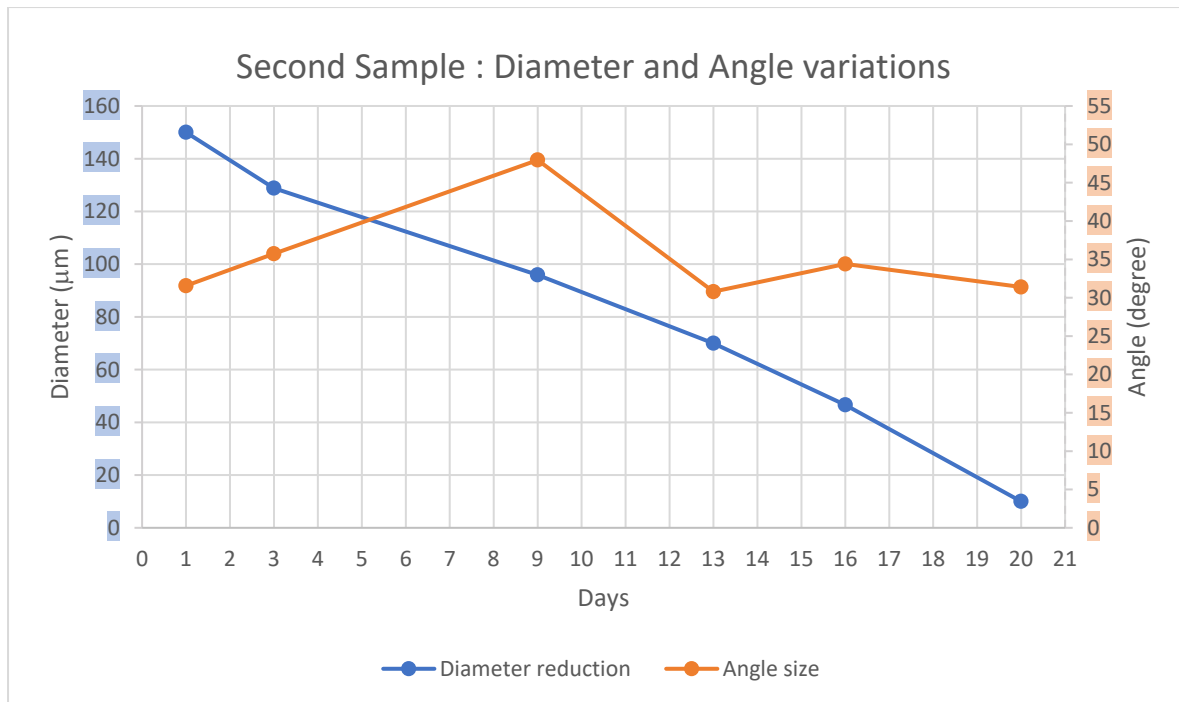
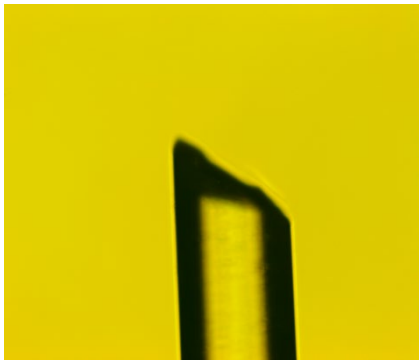
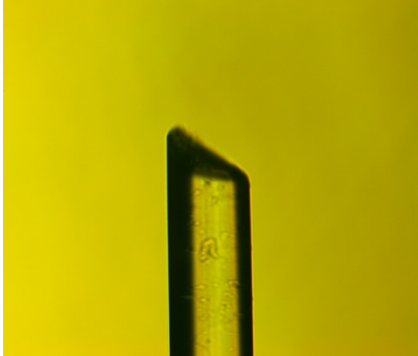
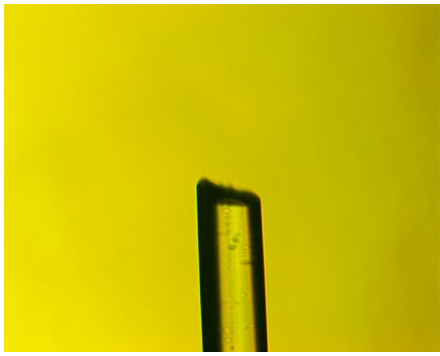
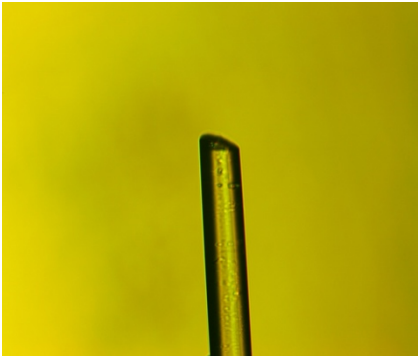
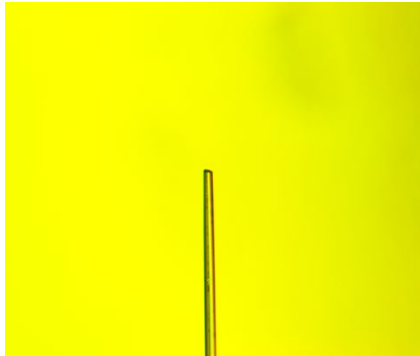


Figure 47: Plot of diameter and angle reduction in a volume of 100 mL of PBS

The third and last fiber sample's cleaved tip was instead obtained imposing a rotation of the cleaver machine's right clamp of **90 degrees**.

<i>Days of immersion</i>	<b>Day 0</b>	<b>Day 3</b>
<i>Pictures of fibers tips</i>		
<i>Angle size</i>	37,01°	35,35°

<i>Days of immersion</i>	<b>Day 9</b>	<b>Day 13</b>
<i>Pictures of fibers tips</i>		
<i>Angle size</i>	35,33°	24,37°

<i>Days of immersion</i>	<b>Day 16</b>	<b>Day 20</b>
<i>Pictures of fibers tips</i>		
<i>Angle size</i>	34,30°	33,53°

The third sample, as the others, didn't show great changes during the days it remained soaked in PBS solution. On **day 9** it actually started showing a small roundness on its previously very pointed tip which was maintained over the rest of the days while the diameter, so the tip of the fiber, was proportionally reducing. On **day 13** the sample had lost completely its sharpness becoming almost flat, with a great angle reduction.

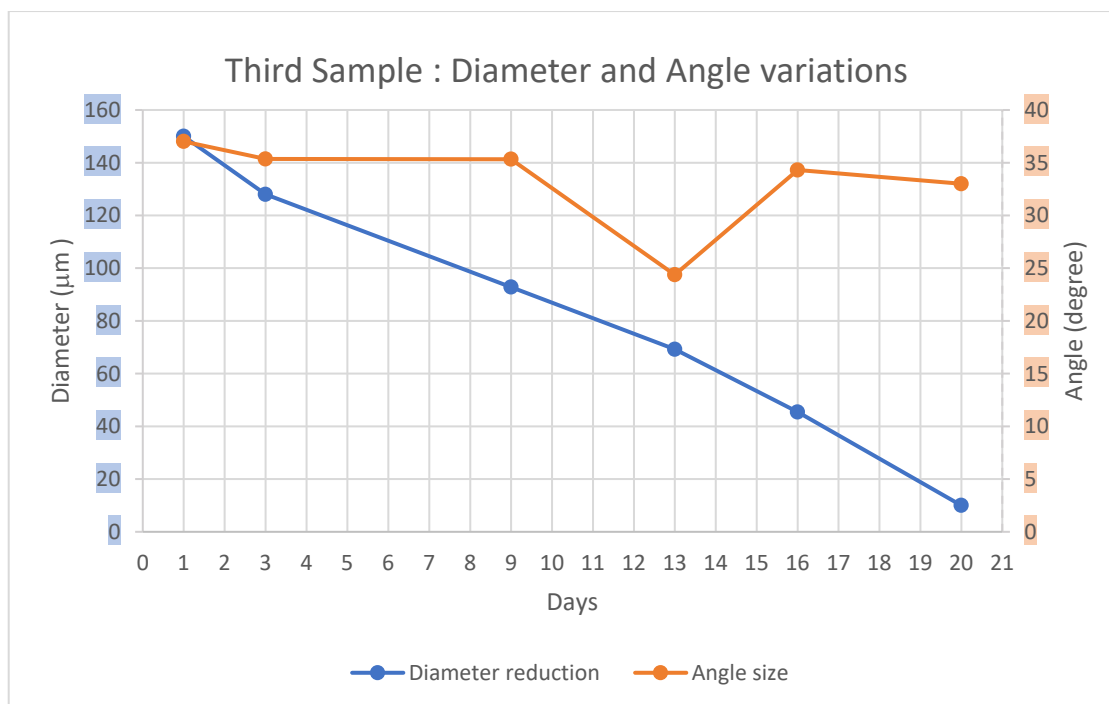


*Figure 18: Plot of diameter and angle reduction in a volume of 100 mL of PBS*

The results of the angle cut study on the fiber samples showed that nevertheless the degradation and the diameter reduction, the tips of the fiber are not so much effected in their shape by the dissolution process. In the graphs is visible how the angle size maintain almost the same value for each day of measure.

Since for the angle cut study of the fiber tips the solution volume/samples exposed area was of  $3.53 \text{ ml mm}^{-2}$ , the dissolution rate obtained for the fiber was of  $7 \text{ µm}$  per day.

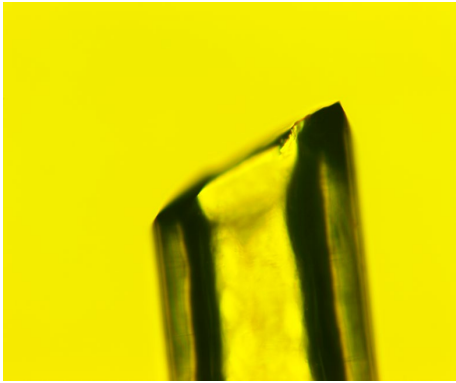
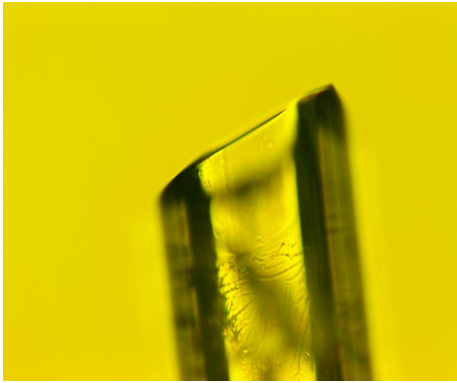
### CALCIUM PHOSPHATE HOLLOW FIBER ANGLE CUT STUDY RESULTS

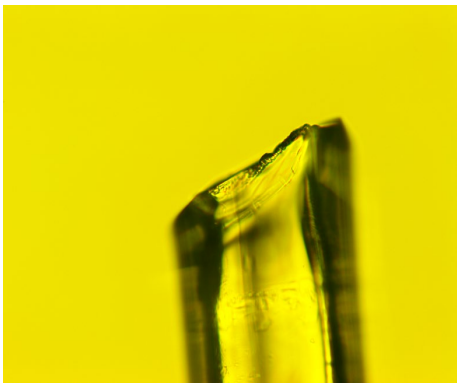
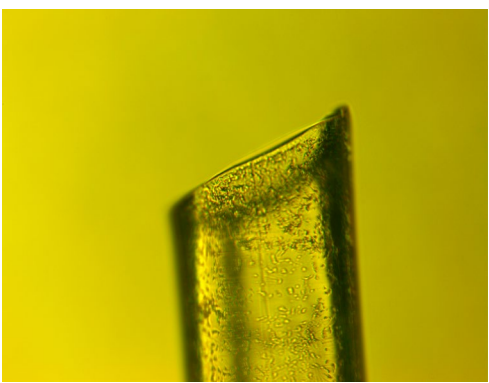
The angle cut study on calcium phosphate hollow fiber was performed in the same way as for the fiber, following the same procedure but leading to partly different and partly similar results.

This was expected because of the intrinsic difference of structure of the two fibers and also because, from the previous dissolution study, a different dissolution kinetics had emerged and that would inevitably have repercussions on the reported type of degradation of the hollow fiber tips.

The hollow fiber angle cut study was interrupted before the fiber one because at day 13, all the samples were broke at their tips. .

The first hollow fiber sample, whose results will be discussed, is the one created with a rotation of the right clamp of **45 degrees**.

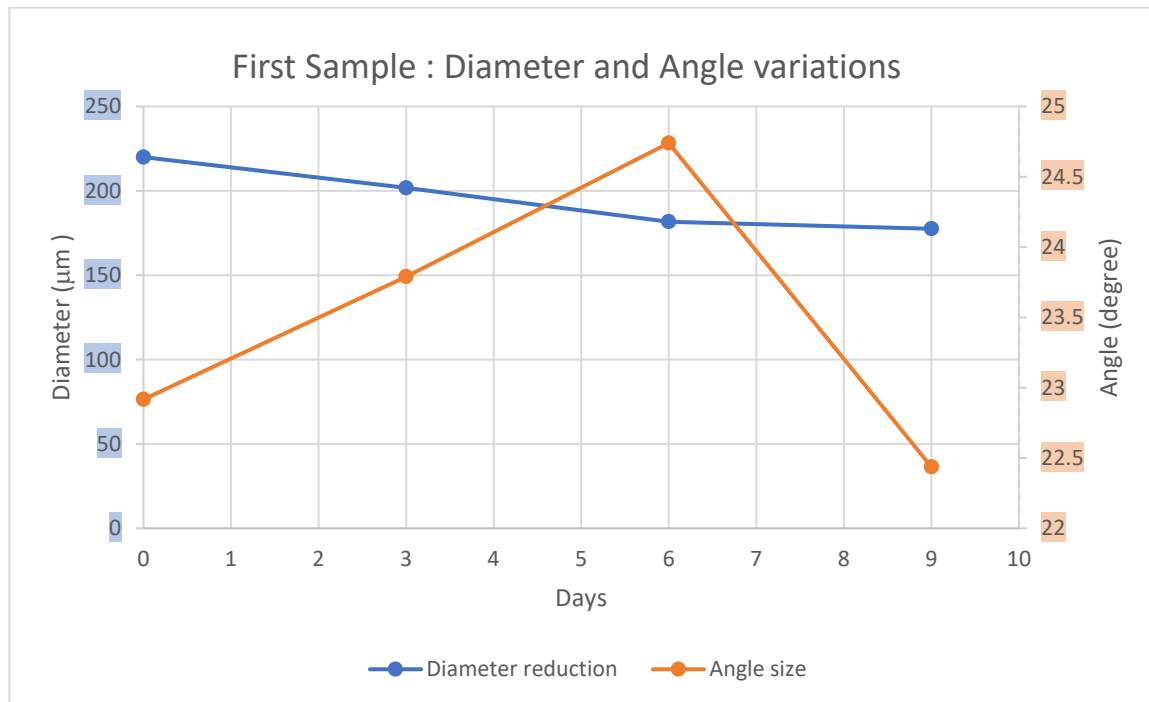
<i>Days of immersion</i>	<b>Day 0</b>	<b>Day 3</b>
<i>Pictures of hollow fibers tips</i>		
<i>Angle size</i>	22,91°	23,79°

<i>Days of immersion</i>	<b>Day 6</b>	<b>Day 9</b>
<i>Pictures of hollow fibers tips</i>		
<i>Angle size</i>	24,74°	22,43°

As for the fiber, also for this hollow fiber sample, we can observe how the PBS solution and the degradation of the tip profile is not so marked, in the first days of immersion, to be effective in reducing the stiffness of the sample.

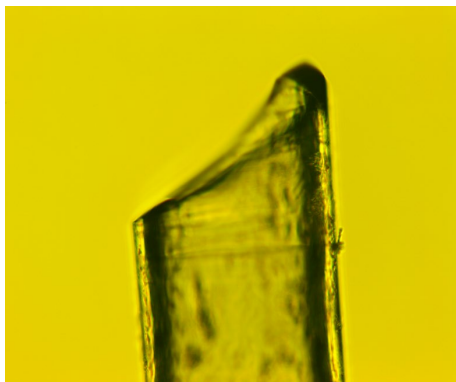
Before to observe any change, the hollow fiber lost the section that was soaked in the solution.

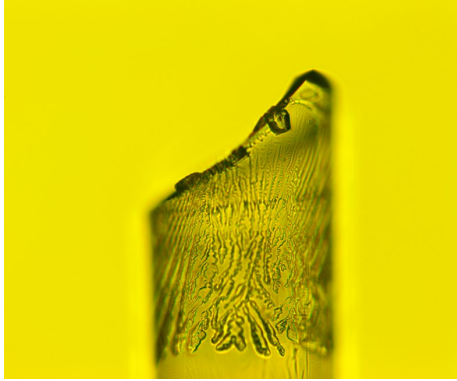
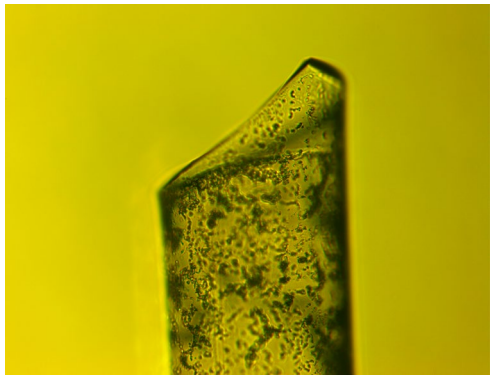
The wall reducing in thickness from the outside and from the inside caused the breakage of the soaked part of the hollow fiber.

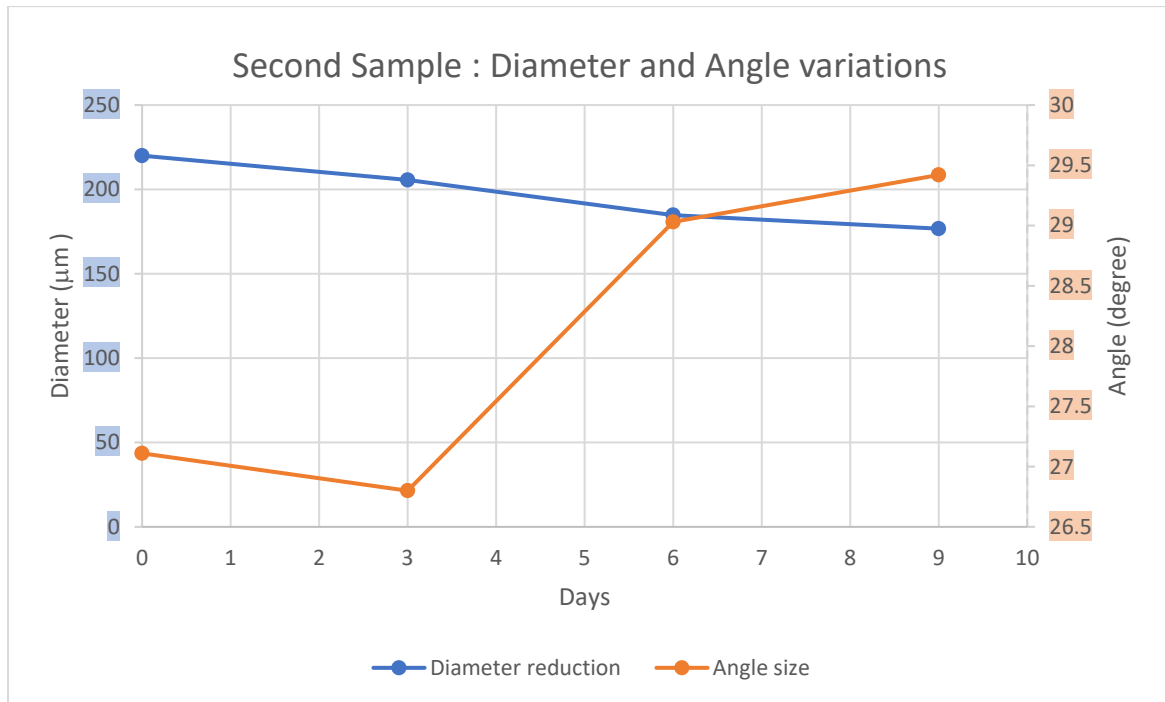


*Figure 49: Plot of diameter and angle reduction of the hollow fiber sample in a volume of 100 mL of PBS*

The second hollow fiber sample was obtained imposing a rotation of the cleaver machine's right clamp of **60 degrees**.

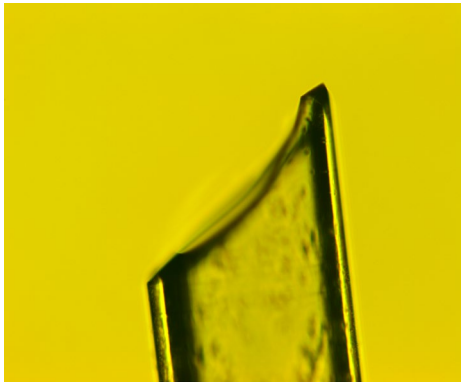
<i>Days of immersion</i>	<b>Day 0</b>	<b>Day 3</b>
<i>Pictures of hollow fibers tips</i>		
<i>Angle size</i>	27,11°	26,8°

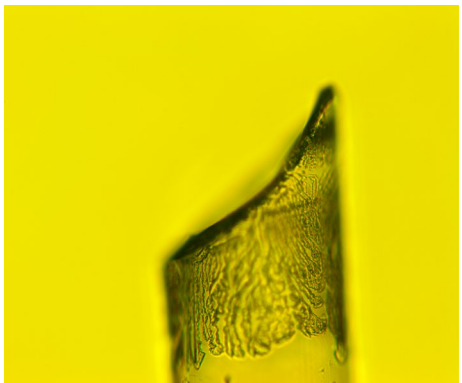
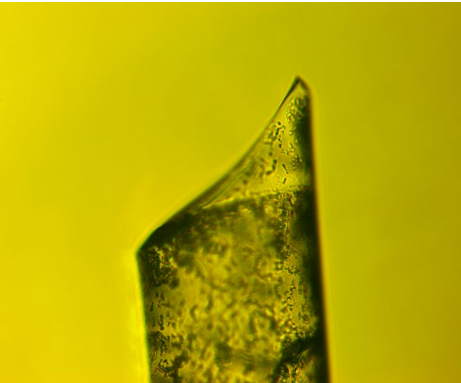
<i>Days of immersion</i>	<b>Day 6</b>	<b>Day 9</b>
<i>Pictures of hollow fibers tips</i>		
<i>Angle size</i>	29,03°	29,42°



**Figure 50** : Plot of diameter and angle reduction of the hollow fiber sample in a volume of 100 mL of PBS

The third sample was obtained imposing a rotation of the right's clamp of the cleaver machine of **90 degrees**.

<i>Days of immersion</i>	<b>Day 0</b>	<b>Day 3</b>
<i>Pictures of hollow fibers tips</i>		
<i>Angle size</i>	30,43°	28,9°

<i>Days of immersion</i>	<b>Day 6</b>	<b>Day 9</b>
<i>Pictures of hollow fibers tips</i>		
<i>Angle size</i>	29,64°	33,87°

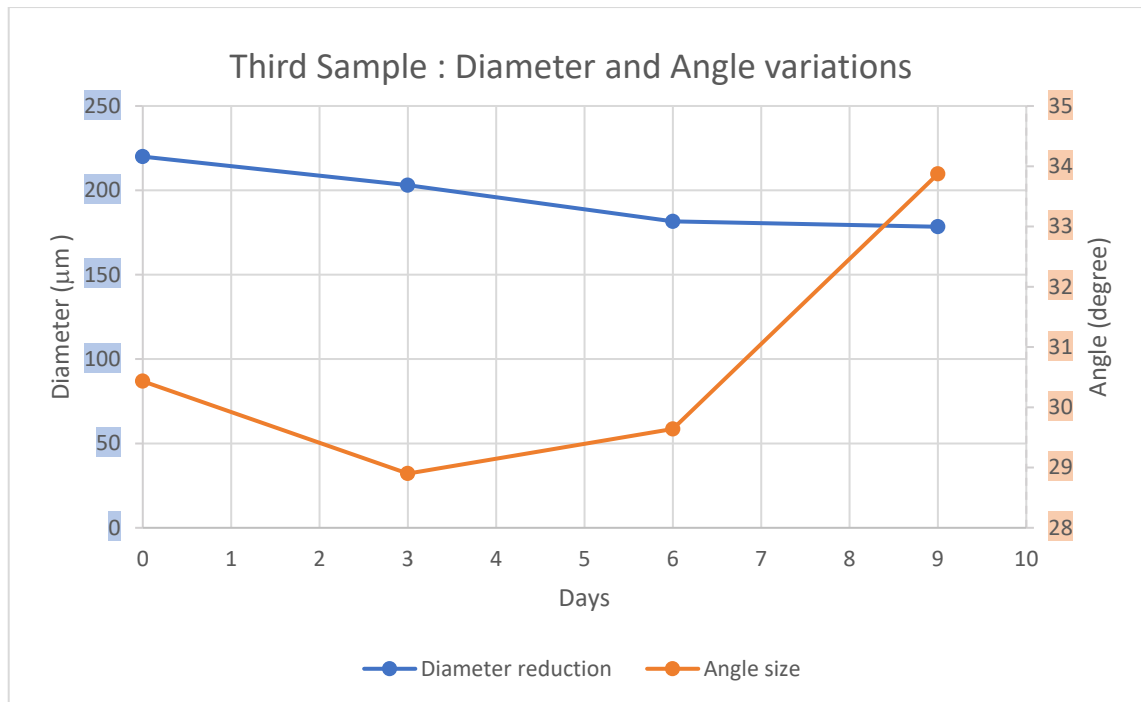


*Figure 51: Plot of diameter and angle reduction of the hollow fiber sample in a volume of 100 mL of PBS*

The second and the third samples, as the first, didn't show big changes in angle size while soaked in PBS solution, but as the first sample, also these ones, experienced breakage on **day 13**.

The dissolution rate obtained with a solution volume/samples exposed area of  $3,61 \text{ ml mm}^{-2}$  was for all the samples of almost  $5 \text{ } \mu\text{m}$  per day. Considering this rate and the thickness of the hollow fiber wall, which was  $55 \text{ } \mu\text{m}$ , degrading from the inside and from the outside, on **day 13**, the tip soaked in the solution was found broke because it was completely dissolved.

The hollow fiber study, confirmed that while fibers and hollow fibers dissolve in PBS and reduce their diameter linearly, the degradation process don't effect their tips shape as expected.

### ***3.3 Transmission test***

The transmission test was conducted on a calcium phosphate fiber whose external diameter was  $150 \text{ } \mu\text{m}$  and the core diameter was  $64 \text{ } \mu\text{m}$ . The test was carried out following the procedure described in **chapter 2.2.3**.

In **Figure 52** is shown the trend of the output power coming from the silica fiber spliced from one end to the calcium phosphate fiber soaked in the PBS solution and

injected through the laser diode at 980 nm of wavelength spliced to another silica fiber spliced to the phosphate one from the other side.

In the picture are shown two trends respective for 80 mA and 100 mA on input current injected using the laser diode controller.

The two trends are coherent respect to each other and shows a decreasing power for both of the injected currents, achieving negligible values of output power on the 21th day when the measures were interrupted manually because none of the values of output power could have been relevant for a biological application.

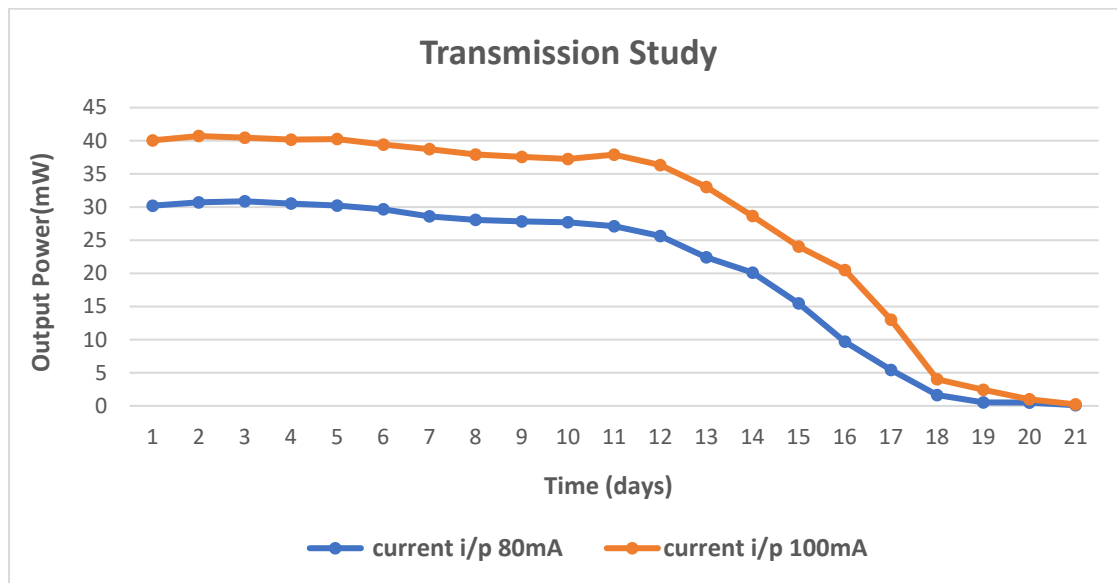


*Figure 52: Output power coming from the silica fiber spliced to the phosphate fiber soaked in PBS solution over the period of 21 days*

From the graph is visible how for the first 10 days the output power is almost constant for both the injected currents. From the dissolution test, we know that in this period of time the fiber is undergoing a slow degradation process but still this diameter reduction of the cladding structure is not affecting too much the transmission of light.

Later on, the output power start to strongly reduce in the last 10 days of trial until it reach the value of almost 0 mW of output.

As observed in the characterization of fiber splice study in **chapter 2.1.2** the light coming out from the same type of calcium phosphate fiber spliced to a multimode silica fiber already spliced to the single mode silica fiber of the laser diode is mostly confined in the core nevertheless the differences in dimensions of the core and the cladding structures of the fibers and the differences in the material, that doesn't allow to obtain a zero loss splice.

The same situation is present, in this case, also on the opposite site of the calcium phosphate fiber, having now two splice and measuring the output power from the multimode silica fiber.

Keeping the silica fibers outside of PBS solution and stack in the same configuration we can conclude that the only factor effecting the transmission of light power is the changing in the coupling of light and its escape from the core of the calcium phosphate fiber soaked in the solution.

The cladding and the core structures with the different refractive indexes, as exposed in **chapter 1.2.1**, are necessary to allow the total internal reflection phenomenon that confine the light in the core. While the fiber reduces its thickness because of its degradation in PBS, the medium where the fiber is soaked which is mostly made of water and has a refractive index of 1.33 is replacing the cladding structure function, since it has always a lower refractive index than the fiber's core one. This allows the fiber to keep transmitting the light reducing the losses.

After the stop of the study the fiber was taken out of the container and observed with the optical microscope (**Figure 53**). Its diameter was measured to establish if it had a value that was coherent with the dissolution study. The diameter was actually about few  $\mu\text{m}$ s which is a value really small for what expected from the measurements taken with the dissolution test on the 21th day.

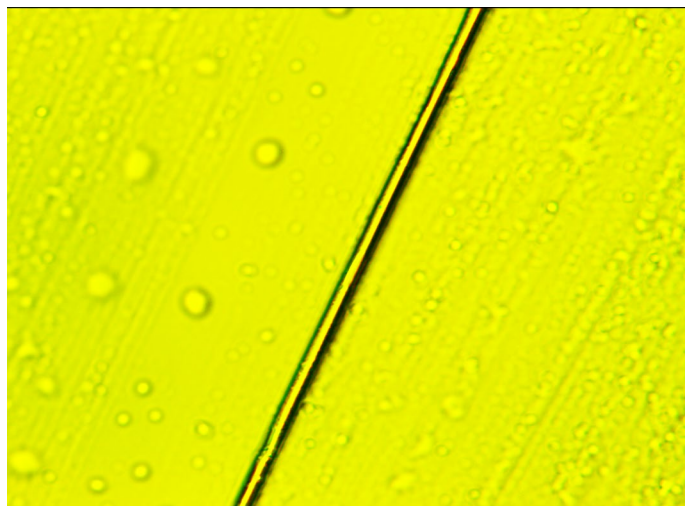


*Figure 53: Optical microscope image of the fiber at the end of the transmission study on the 21th day*

The pH of the solution was measured at the end of the study to assess any change in its value since no refresh of the solution was taken. After 21 days of immersion of the fiber and the thermal sleeves at the splice points in part soaked in the PBS, there was the chance of a change in the pH value. The value measured with the pH meter was 7.3 and still was in the biological range. Excluding the possibility that a changing in the pH value could have effected the dissolution rate of the fiber, we focused on the different volume of solution employed for the transmission and for the dissolution test. We can assume that, in the dissolution test, since the volume was smaller, the solution saturation effected the dissolution speed, reducing it. In the transmission test, the big volume of PBS employed, made the solution saturate later allowing to the fiber to degrade with a rate more constant. Since the diameter

of the fiber, at the end of the transmission study, was about 7-8  $\mu\text{m}$ , considering a constant dissolution rate, we have a reduction in diameter of almost 7  $\mu\text{m}$  per day. With this rate, at the 12<sup>th</sup> day, when it starts the strong decreasing of power transmitted (**Figure 52**), we can assume that, the degradation process, from that moment on, is actually reducing the core diameter.

Further studies for this test could be done modifying the light source, for example using a laser in the visible range to observe any differences in the transmission of light, or changing the setup to allow a more frequent refresh of the medium to mimic better the continuous body fluid exchange.

This could be done using a microfluidic system where the fiber can experience a continuous flow of the degrading solution, with an inlet and an outlet, guaranteeing a dynamic dissolution which is more coherent with the biological condition.

This is actually under study right now, using this new configuration to establish a new protocol for dissolution and transmission study in biological simulated conditions.

To do this, we are using the Elveflow microfluidic system.

The system is composed by a pressure driven flow controller with 2 channels, with an external pressure source which is Nitrogen. The gas exercises a pressure on a sealed PBS reservoir, which makes the liquid flow into the microfluidic channels connected by tubes.

The process is driven by the difference of pressure  $P_{in}$  inside the reservoir and the  $P_{out}$  the outside pressure. If  $P_{in}$  is bigger than  $P_{out}$  the liquid moves from the reservoir to the outlet the opposite happens when  $P_{in}$  is lower than  $P_{out}$ .

The difference of pressure between the pressure of the inlet and the pressure of the outlet is strictly related to the flow rate, which is the amount of liquid passing inside the channel over time, and to the microfluidic resistance which is correlated to the channel and the fluid characteristics.

With a software is possible to set the pressure and adding a flow sensor we can also set the flow rate.

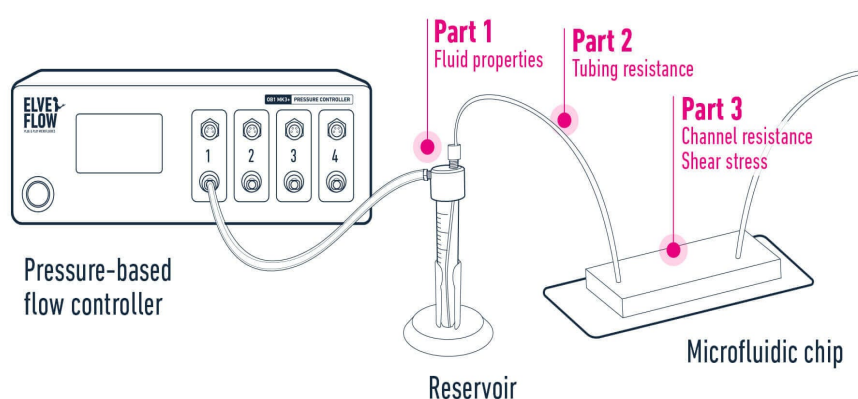


*Figure 54 : Elveflow Microfluidic setup*

The bioresorbable fiber was prepared in the same way of the transmission test, explained in **chapter 2.2.3**, but in this case the phosphate fiber length was different and it was about 4 cm. The fiber was spliced on both end to commercial silica fiber and then one silica fiber was spliced to the light source and the other was used to measure the output power using a power meter.

The light source employed in this case was a fiber coupled LED at a visible wavelength of 554 nm. The temperature was kept to 37 °C using a peltier cell.

After all the processes of splicing the fiber was insert in the microfluidic chips where, at the extremes, there was some parafilm to prevent liquid leaking.

The fiber was blocked inside the chip using some screws, taking care that the bioresorbable fiber was inside the microfluidic channel. The fiber was checked using a usb microscope as shown in **Figure 55**.

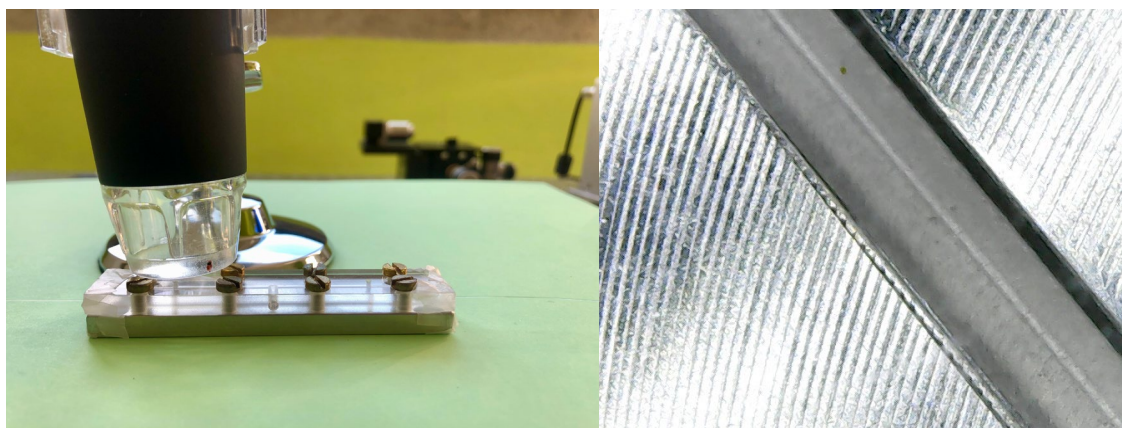


*Figure 55 : Optical fiber inside the microfluidic chip observed with usb microscope*



## 4. Biomimetic phantom for fluorophore release

The last part of this work of thesis was focused on the fabrication of a biomimetic phantom for simulating a drug release using the calcium phosphate hollow fiber. How previously said, the hollow fiber is a very interesting structure for future uses in the biomedical field. The ability of both delivering light and drugs, combine, in one structure, two main therapeutic applications that nowadays are employed for cancer treatment and many other pathologies.

Focusing on the drug delivery feature, it is important to underline how targeted delivery system have gained a growing interest in biomedical treatments for their ability of transporting drugs to specific site of the body avoiding effect on other organs and tissues.

Moreover, the drug delivery system needs to be designed in order to avoid the biological barriers that prevent the drug to reach the target site.

The hollow fiber can overcome these issues reaching deep tissues non invasively and delivering the drug in the specific site of interest.

### 4.1 The fluorophore molecule

The calcium phosphate hollow fiber was employed in this study for the delivery of a fluorophore molecule. Fluorophores are chemical compounds that when excited with a specific light source re-emit light. These molecules absorb photons to a certain wavelength and re emit photons of lower energy, which means of a longer wavelength. They are often used for fluorescence imaging in deep tissues, as molecule sensors and in immunofluorescence.

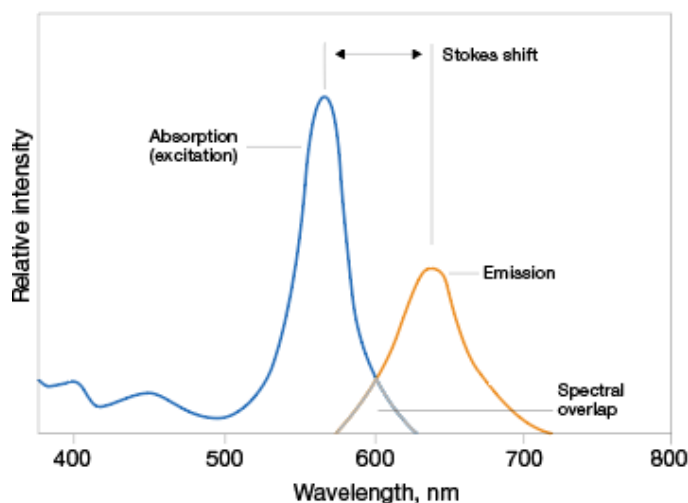


*Figure 56: Example of fluorophore absorbance and emission wavelength range*

As shown in **Figure 56** fluorophore have two different range of wavelength for excitation and emission of light energy.

The first, of shorter wavelengths, is the range in which the fluorophore molecule absorb the light and is excited. The peak of this range correspond to the wavelength which is most likely to cause the excitation with the highest level of intensity.

The second range is the emission one which behaves in a similar way. The maximum of this range correspond to the maximum output intensity of emission.

The Stokes shift is due to some energy loss of the excited fluorophore because of molecular vibrations. The spectral overlap correspond to the range in which the fluorescence overturn so it is better not to excite the molecule in this range because it could be difficult to distinguish the emission.

The fluorophore chosen for the future release test was the Crystal violet.

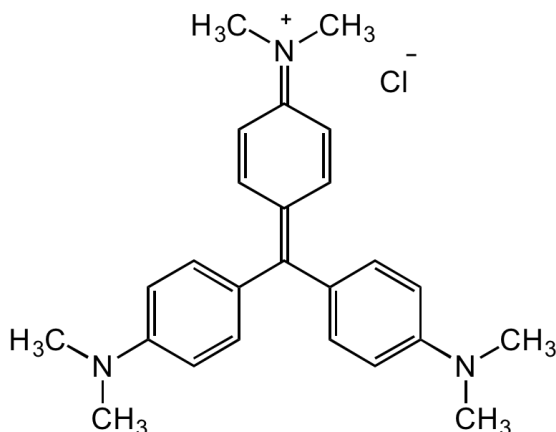


*Figure 57 : Crystal violet structure*

Crystal violet is a triarylmethane dye commonly used as histological stain and for classifying bacteria. It has antibacterial, antifungal and antitumor properties.

The dye dissolved in water has a blue-violet colour and has an absorbance maximum at 590 nm and an extinction coefficient of 87,000 M<sup>-1</sup> cm<sup>-1</sup>.

The color, so the absorption maximum value, it's strictly correlated to the medium where the dye is dissolved.

In fact, crystal violet is also employed as pH indicator moving from yellow color to violet at a transition pH of 1.6.

In **Figure 58** are show the two range, absorbance and emission of the crystal violet fluorophore. The absorbance maximum is at 590 nm which is orange while the emission maximum is 636 nm and the range goes from orange to red.

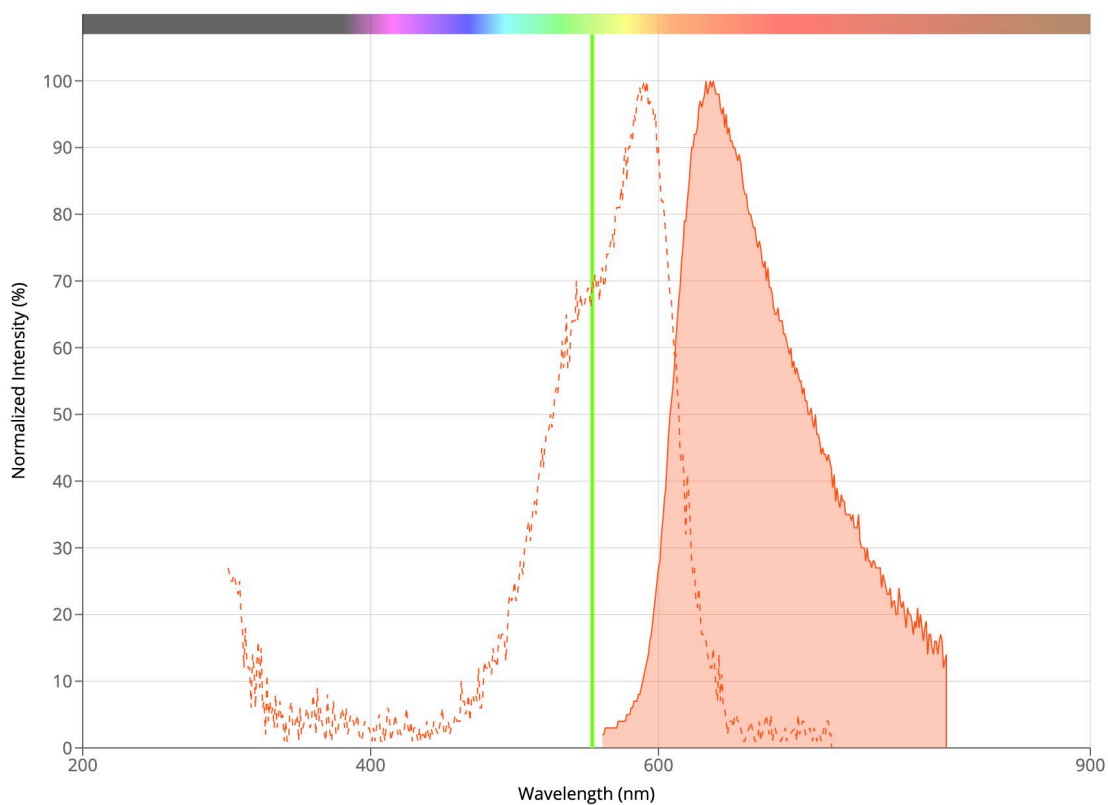


*Figure 58 : Crystal violet absorbance and emission range. The green line indicate the light source wavelength employed to excitate the dye.*

The green line on the excitation range correspond to the specific wavelength chosen in this work to excitate the dye. The light source employed was a fiber coupled LED at 554 nm with a minimum output power of 21 mW and a maximum of 28 mW.

## 4.2 Fabrication of the biomimetic phantom

The phantom fabrication process started with the design of a blood vessels with an apposite software named Autodesk Fusion 360. This is a cloud-based 3D modeling software platform for the design and manufacturing of products.

The blood vessels were designed to have a diameter ranging from 5 mm to 8 mm with a thickenss value varying from 1 mm to 1.5 mm.

The vessels were designed to vary their diameter during their length so to mimic better the real conditions inside the human body.

The dimensions of the vessels were chosen taking into account different aspects like:

- The 3D printer resolution
- The cleaning methods employed to remove the excess of the resin, especially inside the holes.

Starting from the 3D printer used , this was the formlabs Form 3L.

This printer uses the Low Force Stereolitography (LFS) process to print large and quality parts. LFS is an advanced form of SLA technology which uses linear illumination and a flexible tank to transform the liquid resin in new components.

The flexible tank guarantee a low force exerted on the parts during the printing compared to the previous SLA technology .

As the previous technology also LFS is an additive manufacturing process which uses a UV laser on a bath of photopolymer resin. The laser is used to realize, on the surface of the bath, the the component shape programmed using a CAD software .

When the ultraviolet light hit the liquid photopolymer resin this solidify creating a layer. The final object is a set of resin layers that can be constructed horizontally or vertically.

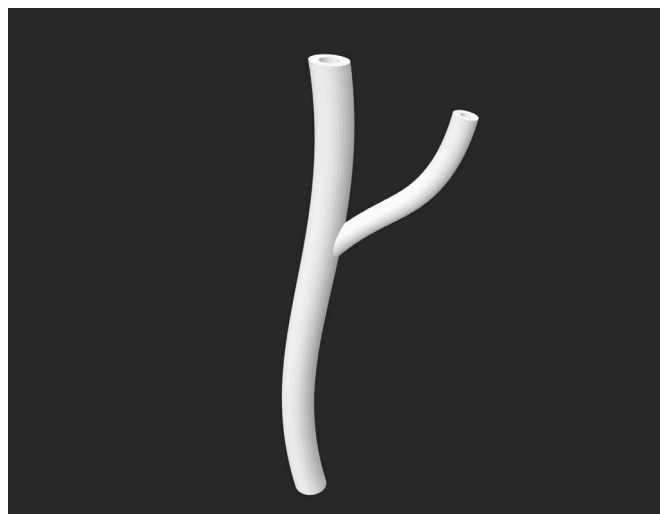


*Figure 59 : Vessels Phantom*

The printer has a layer thickness which means an axis resolution going from 25 to 300 microns and it is equipped with 2 laser source of 250 mW of power. The lasers wavelength is 405 nm, in the UV range, for hardening the photopolymer resin when exposed to the light cross linking the different polymer chains.

The polymer resin chosen to print the phantom was the formlabs Elastic 50A.

This resin is soft and flexible and is chosen to print component that needs to bend without breaking and for models and medical devices.

The resin is transparent, which make it suitable for medical models and also to observe better the emission of the fluorophore.

After printing the object requires a post processing.

To start, the phantom must be washed to remove the excess of resin in the surface and especially inside the holes of the vessels that must be free.

The phantom was soaked in a solution of isopropyl alcohol and the solution was insert in the channels to stop the resin from curing and blocking the channels.

At the end, the phantom was washed with water.

Later, the phantom undergoes a process of curing to increase the stability of the structure. The curing process is the key to reach the optimal strength and mechanical stability of the 3D printed object using UV light and heat to complete the polymerization of all the piece. The laser used for curing has the same wavelength of the printer employed, so 405 nm.

The Elastic 50A resin needed a curing time of 20 minutes at a temperature of 60 °C.

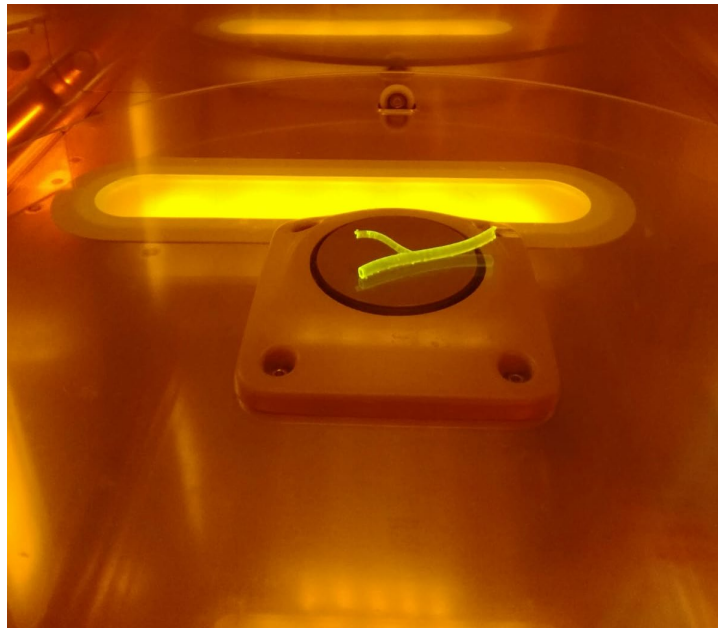


*Figure 60 : Curing process of the phantom*



## 5. Conclusion

This work of thesis had the aim to characterize, in a simulated biological environment, fibers and hollow fibers made of a novel material, with unique characteristics, which was the calcium phosphate glass. This particular material, able to be completely resorbed in aqueous media, without the release of any toxic substances, was chosen to manufacture bioresorbable and biocompatible fiber and hollow fiber samples.

The optical processes of cleaving and splices of the fibers were deeply studied in order to obtain low losses in hybrid splice between the commercial silica fibers and the calcium phosphate fibers and hollow fibers, taking into account the different melting temperatures of the two type glasses. The splice process was optimized to achieve a good guidance of light in the calcium phosphate fiber's core and in the calcium phosphate hollow fiber's wall.

The characterization of fiber splice study demonstrated good results in the guidance of light for the fiber samples, with a splice loss of 0.28 dB. The same study, on the hollow fiber samples, demonstrated that no matter a good guidance in their wall, the losses were very high, and this is mainly due to the structure of this fiber, with no core.

Still, these values can find further improvements in future by controlling the inhomogenities in the glass structure and possible defects at the interface between core and cladding.

The characterization in PBS solution was performed to investigate the optical and the biological features of these fibers and glasses, maintaining a temperature of 37° and a pH of 7.4.

The dissolution test performed on the fiber samples showed that, with the conditions imposed, they completely dissolve in more or less 30 days. The hollow fibers instead, with a hole in their structures have a much faster degradation and dissolve in the third week of immersion.

The angle cut study on both type of fibers showed that tips, with a sharp edge, degradate maintaining the same shape and don't show an enhanced roundness after a few days of immersion. After day 10, a small roundness was visible in some fiber samples tips.

The transmission study on the calcium phosphate fiber allowed to assess the ability of the fiber to transmit light, while soaked in PBS, for 21 days. The power transmitted remained stable in the first two weeks, when the cladding was degrading, while it strongly got reduced when the core has started to reduce its diameter achieving an almost zero output power when the core had a diameter of 7-8  $\mu\text{m}$ .

The different dissolution rate obtained in all the tests performed, where the only condition that was always different was the volume of PBS employed, allowed to understand that the fiber degradation process is strictly correlated to the amount of volume of the solution and to its refresh. When the solution saturate the dissolution rate slow down, this is why, in the dissolution test, the rate increases when the

solution is refreshed and the surface exposed reduced during the previous days of immersion. In a big volume, instead, the saturation process of the solution is slower and the degradation maintain an almost constant rate as shown for the angle cut study. These considerations brought to the realization of a new protocol for testing the dissolution process of these fiber that was able to take into account different aspect such as:

- The need of a dynamic dissolution process, since the body is the furthest thing from being static,
- A continuous flow of the solution which could avoid its saturation process to slow down the degradation rate,
- A flow rate with a value which can simulate the flow per minute inside a specific organ or tissue.

For these reasons, the microfluidics will be employed to perform the dissolution and the transmission tests again.

The realization of a phantom for the release of a fluorophore and its excitation was carried out to demonstrate the ability of the hollow fiber in delivering drugs.

The excitation of the fluorophore could be performed with both hollow fiber or fiber, since it was demonstrated that the hollow fiber can guide light through its wall. This work was preliminary to the effective release of the fluorophore with the hollow fiber since the practical application required more time to be handled and because of problem with the light source.

## 6. References

- [1] R. F. de Mestral, "Calcium phosphate glasses and glass-ceramics for medical applications," *Journal of the European Ceramic Society*, 1989.
- [2] J. M. C. J. C. Knowles, "Phosphate based glasses for biomedical applications," *Journal of Materials Chemistry*, 2003.
- [3] F. R. A. N. E. G. D. A. I. H. K. Islam MT, "Bioactive calcium phosphate-based glasses and ceramics and their biomedical applications: A review.," *J Tissue Eng*, 2017.
- [4] R. D. W. M. K. J. Ahmed I, "Antimicrobial effect of silver-doped phosphate-based glasses.," *J Biomed Mater*, 2006.
- [5] I. Ahmed, H. Ren and J. Booth, "Developing Unique Geometries of Phosphate-Based Glasses and their Prospective Biomedical Applications," *Johnson Matthey*, 2019.
- [6] J. M. P. G. A. N. B. A. K. N. L. K. J. V. H. J. G.-M. J. C. K. S.-Y. B. E. V. a. D. C. Farzad Foroutan, "Antibacterial Copper-Doped Calcium Phosphate Glasses for Bone Tissue Regeneration," *ACS Biomaterials Science & Engineering*, 2019.
- [7] K. J. L. G. K. J. K. H. S. Y. H. J. Joo NY, "Effects of phosphate glass fiber-collagen scaffolds on functional recovery of completely transected rat spinal cords," *Acta Biomater*, 2012.
- [8] G. N. J. L. D. M. S. R. M. F. C. Vitale-Brovarone, " Phosphate glass fibres and their role in neuronal polarization and axonal growth direction," *Acta Biomaterialia*, 2012.
- [9] J. L. D. M. C. V.-B. G. Novajra, "Resorbable hollow phosphate glass fibres as controlled release systems for biomedical applications," *Materials Letters*, 2013.
- [10] C. P. ., D. P. ., N. B. ., N. G. B. ., C. B. ., S. V. ., D. M. Edoardo Ceci-Ginistrelli, "Drug release kinetics from biodegradable UV-transparent hollow calcium-phosphate glass fibers," *Materials Letters*, 2017.
- [11] R. Nazempour, Q. Zhang, R. Fu and X. Sheng, " Biocompatible and Implantable Optical Fibers and Waveguides for Biomedicine," *Materials*, 2018.
- [12] S. G. M. H. M. e. a. Nizamoglu, "Bioabsorbable polymer optical waveguides for deep-tissue photomedicine.," 2016.

- [13] M. A. C. O. M. P. M. M. B. C. A. B. T. N. B. M. A. R. M. J. M. W. M. I. E. K. P. R. W. R. P. T. Shane Johnson, "Photochemical Tissue Bonding: A Promising Technique for Peripheral Nerve Repair," 2007.
- [14] D. Chen, L. Huo, H. Li and G. Song, "A Fiber Bragg Grating (FBG)-Enabled Smart Washer for Bolt Pre-Load Measurement: Design, Analysis, Calibration, and Experimental Validation," 2018.
- [15] F. B. F. T. S. T. C. a. G. A. Chiavaioli, "Biosensing with optical fiber gratings," 2017.
- [16] "Fiber Optic Basics," [Online]. Available: <https://www.newport.com/t/fiber-optic-basics>.
- [17] K. Boyini, "Transmission of Light Through Fiber," [Online]. Available: <https://www.tutorialspoint.com/Transmission-of-Light-Through-Fiber#>.
- [18] "Mode coupling in large-diameter multi-mode silica optical fibers," [Online]. Available: [https://www.researchgate.net/figure/Numerical-aperture-of-optical-fibers\\_fig5\\_258812672](https://www.researchgate.net/figure/Numerical-aperture-of-optical-fibers_fig5_258812672) [accessed 2 Oct, 2022].
- [19] W. contributors, "Optical fiber," [Online]. Available: [https://en.wikipedia.org/w/index.php?title=Optical\\_fiber&oldid=1110319951](https://en.wikipedia.org/w/index.php?title=Optical_fiber&oldid=1110319951).
- [20] "OPTICAL FIBER LOSS AND ATTENUATION," [Online]. Available: <https://www.fiberoptics4sale.com/blogs/archive-posts/95048006-optical-fiber-loss-and-attenuation>.
- [21] "Passive Fiber Optics," [Online]. Available: [https://www.rp-photonics.com/passive\\_fiber\\_optics7.html#:~:text=Usually%2C%20the%20propagation%20losses%20are,attenuation%20coefficient%20in%201%2Fkm..](https://www.rp-photonics.com/passive_fiber_optics7.html#:~:text=Usually%2C%20the%20propagation%20losses%20are,attenuation%20coefficient%20in%201%2Fkm..)
- [22] B. Tanna, "What is Optical Fibre Splice Loss?," [Online]. Available: <https://www.stl.tech/blog/what-is-optical-fibre-splice-loss/#:~:text=When%20it%20comes%20to%20mating,to%200.5%20dB%20per%20splice..>
- [23] D. P. G. B. G. N. A. A. L. C. V.-B. S. A. a. D. M. Edoardo Ceci-Ginistrelli, "Novel biocompatible and resorbable UV- transparent phosphate glass based optical fiber," 2016.
- [24] E. C. Ginistrelli, *Advanced applications of phosphate glass optical fibres in photonics and biophotonics*, Torino : Politecnico di Torino, 2018.
- [25] D. R. Paschotta, "Cleaving of Fibers," [Online]. Available: [https://www.rp-photonics.com/cleaving\\_of\\_fibers.html](https://www.rp-photonics.com/cleaving_of_fibers.html).

- [26] "What Are The Steps Of Fiber Optic Fusion Splicing?," [Online]. Available: <https://www.splicemarket.com/blogs/news/what-are-the-steps-of-fiber-optic-fusion-splicing>.
- [27] "Laser Splicing System LZM series," [Online]. Available: <https://www.fusionsplicer.fujikura.com/products/laser-splicing-system-lzm-series/>.
- [28] W. contributors, "Phosphate-buffered saline," [Online]. Available: [https://en.wikipedia.org/w/index.php?title=Phosphate-buffered\\_saline&oldid=1068956227](https://en.wikipedia.org/w/index.php?title=Phosphate-buffered_saline&oldid=1068956227).
- [29] C. Holler, *Fondamenti di Chimica Analitica di SKOOG & WEST*, Edises.
- [30] K. I. M. ., X. C. Z. ., S. M. B. ., R. E. C. Reece N. Oosterbeek, "Non-linear dissolution mechanisms of sodium calcium phosphate glasses as a function of pH in various aqueous media," *Journal of the European Ceramic Society*, 2021.
- [31] B. Bunker, G. Arnold and J. Wilder, "Phosphate glass dissolution in aqueous solutions," *Journal of Non-Crystalline Solids* 64, 1984.
- [32] Irving, "How to Realize Multimode to Single-Mode Fiber Conversion?," [Online]. Available: <https://community.fs.com/blog/how-to-realize-multimode-to-single-mode-fiber-conversion.html>.



## 7. Acknowledgements

Vorrei iniziare ringraziando il mio relatore: il professore Davide Janner del dipartimento DISAT per avermi dato la possibilità di far parte di questo progetto e per la guida in questi mesi.

Ringrazio la Dott.ssa Nadia Boetti per i preziosi consigli e la supervisione costante durante tutto il lavoro di tesi. Ringrazio il dottorando Jawad .T. Pandayil con cui ho condiviso questo percorso, non sempre facile, tra le gioie e gli scleri con la splicer. In generale, vorrei ringraziare tutte le persone della Fondazione Links e del dipartimento DISAT del Politecnico di Torino che, direttamente o indirettamente, ci hanno aiutato in questo lavoro.

Adesso inizia la parte strappalacrime.

Per primi in assoluto, un grazie ai miei genitori e a mio fratello Marco.

Grazie di avermi sempre incoraggiato, di aver gioito con me ad ogni esame superato e di aver condiviso con me persino l'ansia pre-esame (soprattutto tu, mamma). Non mi avete mai fatto mancare nulla, nonostante il mio essere un 'turbo' ;-), non ve lo dico spesso ma vi voglio tanto bene. Questo traguardo è mio ma soprattutto vostro. Marco, amore, tu non hai fatto granché ma ti ringraziamo lo stesso perchè sei il mio fratellino e ti adoro.

Ringrazio il mio ragazzo, Luca. In questi anni, sei stato il mio riferimento e credo, il mio sostenitore più grande. Grazie della fiducia e di aver sempre creduto in me, forse anche troppo delle volte, ma il tuo essere mi ha spinto a non mollare mai. Spero di riuscire ad essere una spalla per te come tu lo sei stato per me e di riuscire a trasmetterti quanto io creda in te. Tu sai.

Devo dire grazie anche a tutta la tua famiglia. Siete stati sempre molto dolci con me, mi avete accolto e per questo siete stati la mia seconda famiglia. Vi voglio bene.

Grazie alle mie amiche di giù: Sara, Jessica e Marti. Siete sempre state un punto di riferimento. Tra risate e molto disagio, anche da lontano, vi sento sempre vicine.

Procedo adesso per ordine: un grazie speciale va a Giulia, Paola e Marco. Siete state le prime persone che ho conosciuto qui e, lontana da casa, siete stati la mia salvezza quando non sapevo neppure cucinare un piatto di pasta o ero in preda al panico. Grazie, vi voglio bene.

Ringrazio tutta la gang del Borsello : Mous, Lea, Michele, Alice, Calo e Stellins. Siete speciali. Con voi ho capito che si può stare bene ovunque se si è con le persone giuste. Non dimenticherò mai le giocate a briscola al settimo piano, i momenti cultura, Mous che tenta inutilmente di svegliarmi al mattino bussando alla porta, i pranzi, i momenti di pazzia (TANTI, con Calo specialmente), ma soprattutto, non dimenticherò il vostro supporto e il vostro esserci sempre. Vi voglio bene.

Ringrazio i receptionists per il supporto psicologico, Residenza Ascolta che mi ha aiutato tanto e mamma EDISU per questi anni stupendi in residenza.

Vorrei chiudere ringraziando tutte le persone che ci sono oggi , le persone che non ci sono più e quelle che sono state solo di passaggio in questo lungo percorso che

mi ha reso ciò che sono oggi. Tutti voi mi avete insegnato qualcosa e per questo vi sono grata.

Adesso è il momento di scrivere nuove pagine e spero di scriverle con tutti voi.